Diversity of magmatism, hydrothermal processes and microbial interactions at mid-ocean ridges

Gretchen L Früh-Green, Deborah S Kelley, Marvin D Lilley, Mathilde Cannat, Valérie Chavagnac, John A Baross

Accepted version 30. Sept. 2022

Diversity of magmatism, hydrothermal processes and microbial interactions at mid-ocean ridges

Gretchen L. Früh-Green[1†], Deborah S. Kelley[2], Marvin D. Lilley[2], Mathilde Cannat[3], Valérie Chavagnac[4], John A. Baross[2]

[1] Department of Earth Sciences, ETH Zurich, Zurich, Switzerland
[2] School of Oceanography, University of Washington, Seattle, Washington, USA
[3] Équipe de Géosciences Marines, Université de Paris, Institut de Physique du Globe de Paris, UMR CNRS, Paris, France
[4] Géosciences Environnement Toulouse, Université de Toulouse, UMR CNRS, Toulouse, France

[†]Corresponding author, email: frueh@ethz.ch

Abstract

Hydrothermal circulation and alteration at mid-ocean ridges and ridge flanks have a key role in regulating seawater chemistry and global chemical fluxes, and support diverse ecosystems in the absence of light. In this Review, we outline tectonic, magmatic and hydrothermal processes that govern crustal architecture, alteration, and biogeochemical cycles along mid-ocean ridges with different spreading rates. In general, hydrothermal systems vary from those that are magmatic-dominated with low pH fluids >300 °C, to serpentinizing systems with alkaline fluids <120 °C. Typically, slow-spreading ridges (rates <40 mm yr^{-1}) have greater variability in magmatism, lithology, and vent chemistry, which are influenced by detachment faults that expose lower crustal and serpentinized mantle rocks. Hydrothermal alteration is an important sink for Mg, Na, sulphate and bicarbonate, and a net source of volatiles, iron and other nutrients to the deep ocean and vent ecosystems. Magma-hosted hydrothermal systems host a vast, hot and diverse microbial biosphere that represents a deep organic carbon source to ocean carbon budgets. In contrast, high pH serpentinizing hydrothermal systems harbour a more limited microbial community consisting primarily of methane-metabolizing Archaea. Continued advances in monitoring and analytical capabilities coupled with developments in metagenomic technologies will guide future investigations and new discoveries in hydrothermal systems.

Website summary:

Oceanic spreading centres are sites of extensive tectonic, magmatic and hydrothermal activity that provide nutrients to the ocean and multifaceted habitats for life. This Review

explores processes governing variations in hydrothermal vents, microbial ecosystems, and global fluxes from ocean ridges.

Key points

1. Spreading rates control variations in heat sources, magma input, and tectonic processes along mid-ocean ridges and influence crustal architecture and hydrothermal processes, providing multifaceted habitats for life.
2. Approximately one third ($7x10^{12}$ to $11x10^{12}$ W) of the global oceanic heat flux ($32x10^{12}$ W) occurs through hydrothermal convection at ridges and ridge flanks. Seawater circulation, hydrothermal alteration, and microbial interactions regulate seawater chemistry and change the composition and physical properties of the lithosphere.
3. Roughly 50% of the global mid-ocean ridges are spreading at rates <40 mm yr^{-1}, where major detachment faults expose lower crustal and upper mantle rocks, creating asymmetric ridge segments with large variability in structure, hydrothermal processes and vent fluid chemistry.
4. Serpentinization decreases bulk density (<2.9 g cm^{-3}) and seismic velocities (Vp < 6 km s^{-1}) of mantle rocks and weakens the oceanic lithosphere along detachment faults. Serpentinization reactions produce highly reduced fluids with high H_2, CH_4 and other organic molecules that provide energy for microbial life.
5. Hydrothermal processes govern global chemical fluxes (such as Mg, Fe, Mn, and volatiles) and provide nutrients (for example, Fe flux ~4-6 x 10^9 mole yr^{-1}) to the deep ocean.

Approximately 0.05 $GtCyr^{-1}$ of organic carbon are estimated to be produced through microbial interactions and oxidation of organic compounds within hydrothermal plumes.

6. Magma-hosted systems host a vast, hot and diverse microbial biosphere in contrast to serpentinizing systems that sustain more limited microbial communities primarily dominated by methane-metabolizing Archaea. Advanced technologies allow better characterization of the genetic makeup and metabolism of microbes and the role of viruses in shaping diversity.

[H1] Introduction

Mid-ocean ridge (MOR) systems extend approximately 60,000 km around the globe and are the most dynamic and continuous tectonic feature on the planet (FIG. 1). On average, about 3.3 km^2 yr^{-1} of new oceanic crust is generated at global spreading centres[1], which account for >70% of the total volcanism and where about 60-70% of the Earth's surface has been produced over the last 160-180 Myr REF.[2]. Mantle melting, volcanism and faulting at MORs drive hydrothermal circulation that allows the transfer of heat, chemical compounds, metals and volatiles **[G]** from the asthenosphere **[G]** to the hydrosphere and biosphere. Approximately 75-80% of the Earth's total heat flux occurs as the oceanic crust ages[3–5] and is most pronounced at ridge flanks[6], where low temperature fluid flow continues off-axis for millions of years and contributes to global biogeochemical cycles[4,7]. It is estimated that the volume of the ocean circulates through the oceanic ridge system in much less than 1 Myr[6].

Spreading centres are one of the most extreme environments on Earth that can support oases of life at high temperatures and thriving in perpetual darkness. Microorganisms obtain energy from magmatic gases and chemical compounds of altered oceanic crust rather than from

light through a process called chemosynthesis [G][8–10]. In turn, many of these microorganisms symbiotically sustain macrofaunal communities that populate hydrothermal vent environments[8]. The microorganisms with the highest known growth temperature on Earth are found within MOR hydrothermal systems[11,12], and investigation of their genetic diversity has changed the current view of the tree of life[13,14].

Only a small percentage of the global seafloor has been investigated, and as such, the deep ocean remains one of the last frontiers on Earth to be explored and directly sampled. Diffuse, low-temperature (6-17°C) hydrothermal vents were first discovered in 1977 at the Galápagos Spreading Centre in the equatorial Pacific[10]. In early 1979, high temperature (> 350°C), low pH [G] fluids discharging from sulphide structures were found on the East Pacific Rise at 21°N, ref.[15], and demonstrated for the first time that seafloor hydrothermal fluids could transport high concentrations of ore-forming elements[16]. Diffuse springs associated with these vents were found to support exotic benthic communities of giant tube worms, clams, and crabs similar to those found at the Galápagos Ridge, which survive through symbiotic relationships with bacteria that oxidize reduced sulphur[17]. These exciting discoveries inspired subsequent multidisciplinary research into MOR systems that brought to light the complex interplay of magmatism, tectonics, hydrothermal circulation and fluid-rock interaction linked to seawater chemistry and life.

Since the first discoveries, more than 500 sites of hydrothermal venting on the seafloor have been identified[18] (FIG. 1). Integrated approaches of targeted drilling, sampling, biogeochemical analyses, seismic experiments, modelling, and real-time observations at ocean observatories (Box 1) are providing fundamental insights about Earth and the evolution of life, and offer unlimited opportunities for new discoveries. In addition to the pivotal discoveries in the late 1970's of exotic ecosystems around hydrothermal vents[8,19], advances have been made in

monitoring earthquakes and volcanic eruptions in real-time and in understanding the extent of the subsurface biosphere. Advanced analytical and microbiological techniques are helping constrain the role of submarine volcanoes in controlling ocean chemistry and give new insights about novel life forms, their metabolic and genetic diversity, and evolution.

This Review provides an overview of tectonic, magmatic and hydrothermal processes that govern variations in crustal architecture, water-rock-microorganism interactions, and hydrothermal fluxes in MOR systems. We summarise key differences among ridges with differing spreading rates that have experienced varying degrees of magmatism and tectonism. This Review is not intended as a comprehensive compilation of all major sites. Instead, we focus on a few well-studied examples from the East Pacific Rise (EPR), Juan de Fuca Ridge (JdF) and Mid-Atlantic Ridge (MAR), highlighting variations in geological and biogeochemical processes that result in a diversity of hydrothermal environments and associated ecosystems.

[H1] Variations in MOR spreading

A wide range of geological features form at ocean rifts as lithospheric plates diverge and new crust is created (FIG. 2). The morphology and oceanic crustal architecture **[G]** of MORs, and the hydrothermal systems they host, are governed by differences in magmatic, tectonic and alteration processes, which are directly a function of spreading rates and vary in response to regional tectonic stresses and magma supply. These magmatic and tectonic variations at MORs are discussed in this section alongside how they are monitored.

129 ***[H2] Fast-spreading ridges***

130 Fast-spreading ridges (80-120 mm yr^{-1}) generally have high magmatic budgets and erupt
131 voluminous basaltic lavas that accommodate extension, forming a smooth central, raised axial
132 ridge with little faulting. The EPR (FIG. 1) is the fastest spreading MOR, currently reaching rates >
133 100 mm yr^{-1} near 10° N and 150 mm yr^{-1} near 30° S, Refs.[20,21]. Regions with a continuous input of
134 magma are thought to result in a relatively uniform, layered crustal structure, with volcanic and
135 plutonic rocks that are similar to lithostratigraphy found in some ophiolites **[G]** (such as in Cyprus
136 and Oman). Typically, this general layer-cake stratigraphy, referred to as Penrose-type crust[22],
137 consists of a sequence of pillow basalt and lava flows, sheeted-dykes, and gabbros **[G]** that
138 commonly contain ultramafic cumulates, overlying variably tectonized upper mantle sequences
139 (Fig. 2a).

140 Most conceptual models of fast-spreading ridges are based on geophysical studies of the
141 EPR. These models predict that sub-Moho **[G]** melts feed sills through small dykes and
142 accumulate in a shallow axial melt lens (AML), 1–2 km beneath the ridge axis (FIG. 2a)[23,24]. There
143 are contrasting conceptual models for the formation of the gabbroic lower crust at fast-
144 spreading ridges that predict differences in lower crustal structure and which have different
145 implications for thermal and magnetic properties and hydrothermal cooling. Two leading models
146 invoke either: crystallization of multiple stacked magmatic sills (referred to as the sheeted sill
147 model; FIG. 2a); or the presence of one small sill at the base of the sheeted dyke complex from
148 which gabbro cumulates crystallize and subside to form the lower crust (referred to as the
149 gabbro glacier model; see review in REF.[25]).

150 Sheeted sill models predict an axial heat flux of ~15 MW km^{-1} and require extensive, fast
151 hydrothermal cooling along a mush zone to remove latent heat of crystallization at the ridge

axis[25]. In contrast, gabbro glacier models predict that most crystallization occurs within the shallow magma sill, with slow cooling and higher axial heat fluxes of ~30 MW km^{-1} through hydrothermal circulation[25]. Microstructural, crystallographic, and petrological data from the lower crust at Pito Deep on the EPR[26,27] support both models and document regional and temporal variations in crystallization, magmatic flow and faulting with depth in the gabbroic sequences but at relatively constant and fast spreading rates[26]. The magnetic structure preserved at Pito Deep also suggests that crustal temperatures remained around 500°C up to ~8 km off axis[27]. The continuous release of latent heat over this broad region would delay the onset of conductive cooling in the lower crust.

High temperature hydrothermal vents at the EPR are fuelled by small, shallow magma chambers (FIG. 2a) and are influenced by frequent volcanic eruptions that occur every 10-20 years (see overview in Ref.[28]). Frequent eruptions can bury young vents and biological communities and result in smaller sulphide structures and fewer vents along the ridge axis. Eruptive fissures and margins of the EPR axial graben provide well-established permeable pathways for hot fluids to ascend through the crust[28]. The EPR 9°50' N area was the first documentation of a seafloor eruption in 1991 and the impact it can have on both vent fluid chemistry and the surrounding water column[29,30]. For example, time-series analyses of vent fluids sampled within a month of the 1991 eruption documented changes in chloride contents, which were dominated by a vapour phase directly after the eruption but showed an increase in chlorinity to greater than seawater values in 3 years or less[31]. Prediction of a repeat eruption in the same area and observation of the microearthquake character of the eruption was recorded by ocean-bottom seismometers in mid-2005 and documented an intense but brief inferred diking event in early 2006[32,33]. Seismic monitoring at the 9°50' N area between 2003 and 2004 also

provided a regional picture of the distribution of tectonic and hydrothermal stresses that control permeability and promote along-axis flow above the axial magma chamber[34].

[H2] Intermediate-spreading ridges

Mid-ocean ridges with intermediate-spreading rates (40-80 mm yr^{-1}) exhibit transitional morphologies, crustal structure, and variations in hydrothermal output. Temporal and spatial variations in magmatism along these ridges result in both magma-rich regions around axial highs and magma-poor regions more influenced by faulting. The best-studied examples are the Juan de Fuca and Gorda Ridge system (900 km in length) and the Galapagos Rift (1700 km in length). Seismic imaging of the Juan de Fuca indicates stacked subaxial magma lenses **[G]** at depths of ~1.7–4.5 km, extending ~1-8 km along axis and which underlie the majority of high temperature vent sites[23].

Axial Seamount on the JdF is the most magmatically active submarine volcano in the NE Pacific (Supplementary Movie 1), where an extensive cabled network of multidisciplinary instruments has been installed and dedicated for 25 years of operation (Regional Cabled Array; BOX 1). It is the first site where stacked magmatic sills were imaged and where the full evolution of an eruption in real-time was captured[35–37]. Long-term measurements of summit inflation and deflation prior to and following seafloor eruptions at Axial led to the first forecasting model for a submarine eruption[38,39].

The Endeavour Segment of the JdF is one of the most vigorously active hydrothermal areas on the global MOR system and has been the subject of numerous multidisciplinary research since the early 1980's[40–44]. Similar to Axial, it is monitored by a cabled array of instruments, implemented by Ocean Networks Canada (BOX 1). Unlike Axial, no historical seafloor eruptions

198 have been detected at Endeavour. However, widespread venting has produced abundant large
199 sulphide chimneys, some of which are the largest sulphide structures ever discovered[44,45]
200 (Supplementary Movie 2).
201
202 ***[H2] Slow- and ultraslow-spreading ridges***
203 Roughly 50-60% of the global MOR system is spreading at rates <40 mm yr^{-1} and extends
204 from the Arctic Ocean, along the entire Atlantic Ocean, and into the southwest Indian Ocean[46,47].
205 Slow (20-40 mm yr^{-1}) and ultraslow (<20 mm yr^{-1}) spreading ridges have rugged topographies and
206 a large variability in exposed and subsurface rock types, magma supply, and tectonic extension.
207 Plate separation is partly accommodated by faulting, resulting in asymmetric axial valleys and
208 large-offset normal faults, called oceanic detachment faults **[G]** , similar to structures in
209 continental extensional settings (FIG. 2b)[48]. In these environments, the interplay of discontinuous
210 magma supply and tectonic processes results in highly heterogeneous oceanic lithosphere **[G]**
211 and exposure of lower crustal and upper mantle rocks, leading to major variations in geophysical
212 properties, structure and geochemistry along and across ridge axes.
213 Oceanic detachment faults **[G]** are recognized as a distinct mode of oceanic accretion and
214 have a key role in fluid circulation[49]. Serpentinized mantle peridotite **[G]** and lower-crustal
215 plutonic rocks exposed through detachment faults represent on average 25% of the seafloor[47,50].
216 Long-lived (>1 million years) detachment systems result in dome-shaped massifs, with spreading-
217 parallel undulations (corrugations) of the seafloor. These corrugated domes, termed oceanic
218 core complexes (OCCs) or megamullions[51,52], are common along the Mid-Atlantic and Southwest
219 Indian Ridges (SWIR)[53–55]. OCCs form in the footwall of axial detachments during periods of
220 reduced and variable magma supply and are juxtaposed to more volcanic seafloor in the

221 opposite plate (FIG. 2b)[56,57]. In some ultraslow-spreading locations, such as the easternmost
222 SWIR and regions of the Gakkel Ridge in the Arctic[56,58,59], very low melt supply results in more
223 extensive, widespread exposures of mantle rocks[56]. Studies of OCCs have documented complex
224 histories of deformation[54,60–62] and fluid circulation[63,64] along the detachment fault zones leading
225 to active hydrothermal systems, such as the high temperature TAG (Trans-Atlantic
226 Geotraverse)[69,72] and the serpentinite-hosted Lost City hydrothermal fields[65,66].
227 The northern MAR is the best studied slow-spreading environment and currently the site
228 of an uncabled seafloor and water-column observatory dedicated to long-term (>20 years)
229 monitoring of volcanic, tectonic, hydrothermal and biological activity at the basalt-hosted Lucky
230 Strike hydrothermal field[67] (BOX 1). Measurements at Lucky Strike have revealed an estimated
231 minimum total heat flux of 200 MW, REFS.[68,69], similar to heat flux estimated at the Costa Rica
232 Rift[70]. Numerical modelling predicts along-axis hydrothermal flow at Lucky Strike[71], which is
233 consistent with more recent seismic studies at 9°50'N on the EPR[34].
234 Multidisciplinary investigations of MORs continue to provide a better understanding of
235 variations in seafloor spreading processes as a function of spreading rate and highlight the
236 complex relationship between magmatic and tectonic processes that influence the formation of
237 volcanic and plutonic crust and exposure of mantle rocks on the seafloor. Differences in
238 magmatic activity and crustal architecture also control seawater circulation, hydrothermal
239 alteration and vent fluid chemistry, which impact hydrothermal fluxes and microbial interactions,
240 and are discussed in the following sections.
241

[H1] MOR hydrothermal systems

Contrary to early assumptions, hydrothermal circulation in the oceanic crust and the distribution and composition of MOR vents are highly variable, and depend on the interplay of tectonic, magmatic, geochemical and biological processes.

[H2] Hydrothermal circulation at MORs

Penetration of seawater is limited in all settings to the depth of the brittle lithosphere, which is a function of spreading rate **[G]** and thermal structure. Permeability in this brittle domain likely decreases with depth, and hydrothermal circulation is expected to be restricted to < 6 km, with the possible exception of the damage zone of axial detachment faults[72]. At fast-spreading ridges, axial magma chambers at depths of 1-2 km drive shallow hydrothermal circulation[24,73,74]. Models of the thermal structure of MORs that fit multichannel seismic data and axial earthquake centroid depths[75] suggest that a steady-state magma lens can only exist at depths < 6 km at spreading rates greater than ~40-60 mm yr^{-1}. As spreading rates decrease, persistent magma bodies are deeper and the permeability of the upper lithosphere becomes more complex, with fluids channelled along normal faults that can reach 5-8 km into the oceanic lithosphere[76]. Therefore, at slower spreading ridges, only transient melt bodies can exist at depth[77,78] and hydrothermal circulation mainly occurs along faults. In the following section, the main types of hydrothermal systems are discussed, but we emphasize that a strict categorization of vent types is not always applicable.

[H2] Types of hydrothermal systems

The type of rocks in the subsurface of hydrothermal systems together with variability in heat sources and faulting have a profound influence on fluid circulation pathways, vent

distribution and fluid chemistry. At least three general classes of vent systems have been distinguished[79] (FIG. 2): high-temperature (>300°C) hydrothermal systems driven by cooling magmas and/or proximal gabbroic crust; high-temperature hydrothermal vents (>300°C) in detachment settings where variable mixtures of gabbro and peridotite influence heat and mass fluxes; and low- to moderate-temperature (<~120°C) hydrothermal activity driven by cooling of mantle-dominated lithosphere resulting in serpentinization **[G]**, alkaline fluids and precipitation of carbonate chimneys (BOX 2), exemplified by Lost City[65,80] on the MAR and Old City on the SWIR[81] (FIG. 2f).

However, not all MOR hydrothermal systems fit directly into these general categories. For example, the ultra-slow Mid-Cayman spreading centre in the Caribbean Sea is the deepest site yet discovered that has multiple hydrothermal vents and likely different sources, all in close proximity at varying water depths[82]. At Mid-Cayman, the vent fluid chemistry and temperatures are intermediate between high and low temperature systems[82–84] (Supplementary Data). The most prominent feature is Mount Dent, a topographic high on the western flank of the axial valley, which hosts multiple vent fields with abundant fauna, including the Von Damm and Piccard vent fields at 2,300 m and 4,960 m, respectively[82]. Mount Dent is interpreted as an OCC and the fluid geochemistry reflects the influence of both gabbroic and ultramafic rocks along the flow and alteration pathways[85]. In contrast to other high-temperature systems, hydrothermal activity at the Von Damm vent field could be supported by deep fissuring on the OCC, allowing heat to be mined from a deep crustal source rather than from cooling of magma at depth[82].

The diversity of hydrothermal systems at MORs reflects variations in heat sources and differences in subsurface rock types. In general, magmatism fuels high temperature hydrothermal systems with variable chemistry that are found in all spreading environments,

whereas deep faulting promotes lithospheric cooling and drives medium to low temperature systems with fluid compositions indicative of interaction with lower crustal and upper mantle rocks exposed on, or close to, the seafloor.

[H1] Vent distribution and chemistry

Sampling and measurements over multiple months and years provide important constraints on regional and temporal variations in seismic activity, hydrothermal circulation, permeability, fluid-rock and microbiological interactions, and how these are affected by tectonic and magmatic events[31,40,86]. The key controls on the distribution of hydrothermal systems and their vent chemistry are discussed in the following sections (FIG. 3).

[H2] Alteration along convection pathways

As seawater-derived fluids penetrate the crust and are heated at depth, convection cells are established, resulting in zones of hydrothermal upflow and fluid discharge onto the seafloor that drive cold seawater downflow and recharge of the system (FIG. 3b). Water-rock reactions along the convection pathway result in chemical exchange that alters the composition of the host rocks and transforms seawater into hydrothermal fluids.

[H3] Basalt-hosted and high temperature systems

The highest temperature and deepest portion of the hydrothermal circulation cell is known as the reaction or root zone[87], although reactions occur over the entire circulation pathway and continue on the ridge flanks. Hydrothermal alteration of the oceanic lithosphere at varying temperatures is an important sink for seawater-derived Mg, sulphate and alkali elements (FIG. 3b), but a source for many others, such as Ca, Cu, Fe, Mn, Zn, Pb, Li, Rb, REE and Cs[31,87]. Volatiles,

such as H_2, CO_2, H_2S and CH_4, can be released through magmatic degassing or form through fluid-rock reactions and can be utilized or produced by microbial ecosystems at and beneath the seafloor[9,42]. At the deepest level of penetration in magmatic systems, water-rock reactions produce greenschist-facies minerals in the reaction zone and acidic hydrothermal fluids, which are enriched in metals and volatiles and are extremely hot: 350° to >400°C (Supplementary Data). High temperature fluids are buoyant and rapidly rise to the seafloor through pipe-like conduits. Mixing of superheated fluids with cold seawater at and near the seafloor causes dissolved metals to precipitate and the formation of variably-sized edifices and sulphide deposits forming black and less commonly white smoker chimneys that have become hallmarks for hot marine hydrothermal systems[28,88] (FIG. 3b).

[H3] Diffuse fluid flow at hydrothermal vents

There are two types of low temperature or so-called diffuse vents that are integral components of magma-hosted hydrothermal environments. One type of diffuse venting occurs in basalts that are too fractured for the flow path to become sealed (as in high temperature vents), and the rising hot fluid mixes with seawater to produce dispersed fluids with temperatures of 5 - ~50°C (FIG. 3b, orange arrows). Geochemical data indicate that such diffuse fluids show a loss of H_2S and H_2, and gain of CH_4 that are not simply dilutions of high temperature vent fluids but point to subsurface microbial interactions[89,90]. The microbial populations associated with such diffuse sites can be spatially distinct but temporally stable[91,92] and likely sustain a subsurface biosphere[93–95]. The other type of low temperature fluid emission is diffuse flow directly within sulphide structures where high temperature fluid mixes with seawater as it moves through the porous walls of the mounds. Both types of diffuse flow support complex microbial and macrofaunal communities that are different from those at vent sites with focussed flow[10,96].

Diffuse fluid flow is also important in slow-spreading environments and influences the alteration of mantle rocks and serpentinization processes. Peridotite-hosted systems have highly complex and variable vent chemistry, which we discuss in more detail in later sections.

[H2] Phase separation

In addition to water-rock reactions, two important processes – boiling and condensation of brines – impact vent fluid compositions in all high temperature environments[97–100] (FIG. 3c). Because seawater contains 3.2 wt% (weight percent) NaCl, it behaves differently than pure water as it is heated[97]. As seawater migrates to depth, at temperatures above 407°C and pressures above 298 bars (2980 m at hydrostatic pressure), the fluids separate into droplets of brine and a lower salinity vapour phase. This process is called supercritical phase separation or brine condensation. These processes partly govern gas concentrations (for example, CO_2, H_2S, and H_2) and are important in partitioning chloride and metals. The development of low-salinity vapours (< 3.2 wt% NaCl) and brines (up to 10 wt% NaCl) by phase separation is inferred to be an active process throughout the oceanic crust and is documented in diverse magmatic rocks (FIG. 3c; Supplementary Data). As hydrothermal systems wane and cool, the brines can be entrained into upwelling fluids (for example, Endeavour fluids reach twice normal seawater salinities) or are released during eruptive events[101,102]. Brines in the subsurface support distinct, high-temperature, anaerobic **[G]** microorganisms (halophiles) that tolerate very high NaCl concentrations and metal-rich fluids[103].

Extreme phase separation was documented at the Turtle Pits and Comfortless Cove hydrothermal fields at 5°S MAR, where 407°C black smoker chimneys were emitting gas bubbles and chloride-depleted fluids (224 mM Cl) with respect to seawater values (545 mM Cl)[104,105]. At

3000 m depth, venting was occurring at pressure-temperature conditions near the critical point of seawater **[G]** salinity fluids. A short burst of fluid (20 seconds) in the Comfortless Cove field was measured at 464°C, clearly above the critical point and far higher than previously measured fluid temperatures (FIG. 3c)[105]. The low-salinity fluids were enriched in Fe, Cu, Co and Mo[106], reflecting the extremely high temperature of the fluids and importance of phase separation and chloride-complexing in metal transport.

High-temperature fluids and their vapour-dominated nature are influenced by volcanic activity[40,107,108]. For example, following a diking event at the Main Endeavour Field in 1999, the 380°C edifice named Puffer at 2200 m was venting fluids with one of the lowest chlorinities ever measured (19 mM Cl). In 1998, a temperature of 405°C was measured at the Brandon Vent on the southern EPR with fluids that varied from below to above seawater salinities[109]. At pressures and depths greater than the critical point of seawater, all vent fluid temperatures fall far off the two-phase curve, many of which occur along the MAR (FIG. 3c; Supplementary Data). Vent temperatures and fluid chemistry suggest that substantial cooling occurs during ascent of the fluids. On the Mid-Cayman Rise, 401°C fluids from the Piccard site are thought to have phase-separated at temperatures in excess of 500°C and deeper within the crust[84].

[H2] Impact of magmatic events

The large volume of melts at MORs is an important reservoir for volatiles and plays a key role in transferring gases such as CO_2 and He from the mantle to the hydrosphere. Perhaps more than any other factor, volatiles provide a common thread that link geodynamic, geologic, and geobiological processes in submarine environments. Pronounced changes in seismic activity, permeability, heat flux, temperature and vent fluid chemistry result from intermittent diking and

volcanic eruptive or tectonic events at MORs[40,86,108,110]. Large increases in CO_2 could precede volcanic events, as documented at the Main Endeavour Field following an earthquake swarm in 1999[40,111,112]. Lava interacting with hydrothermal circulation cells produces extreme changes in water-rock reactions and the nature and degree of phase separation. These events also provide nutrients and energy to microbial populations[113], alter macrofaunal communities, and produce large deep-sea hydrothermal plumes **[G]** in the water column[114].

An important feature of submarine diking-eruptive events is the formation of so-called megaplumes, characterized by the sudden voluminous release of volatiles into the water column, anomalous heat and He relationships, and elevated Mn and Fe that can persist 2-5 years (see review in ref.[42]). The buoyant megaplumes can rise 1000 metres or more above the surrounding seafloor and can be 20 km across and 70 km in length[114,115]. Estimates of the relative heat flux indicate a sixfold increase during eruptions[36]. Magmatic volatiles released during emplacement of melt into water-saturated porous oceanic crust provide nutrients for massive microbial blooms that accompany eruptions[116–119]. Expulsion of microbial floc **[G]** and formation of snowblowers **[G]** was first documented at EPR 9°50’ N[29] and has been observed at Axial Seamount and on the CoAxial segment of the JdF[35]. This snowblower phenomenon likely occurs during and after most diking and/or eruptive events and is the result of explosive growth of sulphide-oxidizing bacteria during mixing of large volumes of hydrothermal fluid with oxygenated seawater below the seafloor. These observations and studies of microbes thriving within low- to moderate-temperature diffuse flow fluids have been key in forming the hypothesis that there is a vast, but largely unexplored, diverse microbial biosphere in the crust in close proximity to volcanoes and active submarine hydrothermal systems[94,121,122].

[H2] Sediment influence

Where ridges are near continental margins, spreading centres can be covered by sediment and are thus classified as sedimented ridges. The presence of a low permeability, insulating blanket of sediment over more permeable volcanic basement directly influences heat and fluid fluxes and the chemistry of the hydrothermal systems that are commonly rich in hydrocarbons[123–125]. The best-studied sedimented MORs are Middle Valley on the JdF[126,127], the Escanaba Trough on the Gorda Ridge[127–129], and the Guaymas and Pescarado Basins in the Gulf of California[124,130,131]. The chemistry of hydrothermal fluids rising through the sediment cover is metal-poor and enriched in CH_4, NH_4, and higher hydrocarbons as a consequence of thermogenic decomposition of organic matter[132] (Table 1; Supplementary Data).

High CH_4 and NH_4 and low values for $\delta^{13}CH_4$[133], as well as elevated B, $\delta^{11}B$, Br, I, Li, Rb, Cs, distinguish Endeavour from many other black smoker systems and led to the concept of a bare-rock, sediment-influenced hydrothermal system[133,134]. The sedimentary component at Endeavour has been hypothesized to be Pleistocene turbidite flows from the Vancouver Island continental margin that are buried at depth[133]. Such turbidite flows buried the Middle Valley hydrothermal site under thick sediments and currently lap to within 200 m of the axial valley at the northern end of the Endeavour segment. Stable and radiocarbon isotope studies[135] showed that sediments also supply a portion of CO_2 to the vent fluids. Another known sediment-influenced vent system is Loki's Castle on the ultraslow-spreading Arctic Ridge, which is also enriched in barium[136,137].

In summary, oceanic spreading centres are sites of variable but extensive hydrothermal circulation that impacts exchange between seawater and the lithosphere and provides nutrients for microbial activity on and below the seafloor. In addition to subsurface lithologies and water-rock-microbe interactions, phase separation and magmatic events are important factors that

influence vent fluid compositions. Crustal architecture, magma supply and hydrothermal activity are particularly diverse at the slow-spreading MAR, as discussed in the following sections.

[H1] The impact of serpentinization

A number of hydrothermal systems along the slow-spreading MAR are hosted in ultramafic and gabbroic rocks. These include the Rainbow (36°N), Logatchev (14°45'N) and Ashadze vent fields (12°58'N)[138,139] and the off-axis Lost City hydrothermal field (30°07'N)[65,80]. These systems vary in venting temperature, fluid composition, and type of hydrothermal deposit, but all characteristically have high CH_4 and H_2, attributed to seawater interaction with gabbroic and ultramafic rocks along the circulation pathways[65,140]. High H_2 concentrations especially mark the influence of serpentinization processes on fluid chemistry[141–144] (BOX 2, Supplementary Data). Such systems with highly reducing H_2-rich fluids have gained particular interest because of the potential for abiotic **[G]** reduction of dissolved inorganic carbon (DIC) to form organic compounds and their potential role in prebiotic chemistry and the origin of life on Earth and perhaps other planets[145–147].

[H2] High temperature peridotite-hosted systems

Key differences between high and low temperature peridotite-hosted systems are observed in pH, temperature and CO_2 contents, which in addition to differences in trace element concentrations and mantle $\delta^{13}C$ values of CO_2[138,148], point to magmatism as an important source of heat and CO_2 at slow-spreading ridges (Table 1). The Rainbow, Logatchev, and Ashadze fields are black smoker systems, in which sulphides are deposited from low-pH (pH ~3.3), high-temperature (350 – 365 °C), metal-rich fluids with high concentrations of CO_2, CH_4, H_2, and higher hydrocarbons[138,140,149] (see figure in BOX 2). Rainbow vent fluids have high chlorinity (above

seawater concentrations) indicative of supercritical phase separation (FIG. 3c) and contain the highest dissolved Fe of any MOR vent fluid yet studied[150] (Supplementary Data). Elevated CH_4 and H_2 in MAR high temperature vents likely reflect a gabbroic and ultramafic influence in the subsurface[140,151,152]. Heat output from Rainbow has been estimated at 1–5 GW[153], which is the largest heat flux yet discovered. High heat and fluid output, the formation of sulphide deposits, low pH, and high CO_2 and Fe concentrations in the fluids all suggest that hydrothermal circulation in high-temperature peridotite-hosted systems is likely driven by crystallizing magma within the lithospheric mantle. A magmatic heat source is consistent with seismically imaged magmatic sills beneath the Rainbow hydrothermal field[154].

[H2] Lost City

The Lost City hydrothermal field on the Atlantis Massif (MAR 30°N) is the first discovered end-member for serpentinite-hosted, hydrothermally active systems devoid of magmatic activity[65,80] and is likely an analogue for the Old City vent field on the SWIR[81]. Lost City is the furthest off-axis submarine venting environment and is dominated by variably altered peridotite with gabbroic lenses in the subsurface[66,155]. The fluids are 40° – 116 °C and alkaline (pH 10 – 11), with very low CO_2 and metal concentrations, and high CH_4, H_2, formate, and higher hydrocarbons[65,156–158] (BOX 2; Supplementary Data). Hydrothermal circulation is thought to be driven by residual crustal heat and lithospheric cooling, with fluid compositions primarily controlled by serpentinization reactions[65,159], and fluid discharge controlled by normal faults[66]. Mixing of the alkaline fluids with ambient seawater produces up to 60 m high, carbonate-brucite towers within the field (FIG. 2f; Supplementary Movies) and carbonate deposits along pre-existing, subparallel deformation structures in the detachment fault zone[65,66,159,160].

Because the hydrothermal carbonate structures are bright white (Figure 2f), the Lost City vents have erroneously been referred to as white smokers. However, white smoker vents are part of evolved, high temperature, basalt-hosted sulphide systems, located distal to the main upflow zone (FIG. 3b) and emit lighter-hued minerals, rich in barium, calcium, sulphate or silicon, leading to the precipitation of anhydrite at temperatures higher than 150°C and barite towards lower temperature[88]. In contrast, the Lost City fluids are clear, commonly diffuse, and essentially devoid of mineral or metal particles (Table 1).

[H2] H_2 export and DIC uptake

Serpentinization has consequences for H_2 fluxes in hydrothermal systems[47,158,160] (BOX 2). Water column studies and in-situ monitoring while drilling across the Atlantis Massif indicate widespread release of H_2 (up to 44nM) into the water column and elevated H_2/CH_4 ratios which are distinct from channelled flow at Lost City[155,160,161]. In addition, radiocarbon data and distinctly low concentrations of CO_2 in the fluids have been used to argue that modern seawater DIC must be lost within the circulation paths, likely deposited as carbonate in the basement rocks[156,162,163]. A similar uptake of seawater bicarbonate was documented at Endeavour[135] and at 9°50'N, suggesting that hydrothermal systems in general could be an important sink of DIC from seawater, stored as carbonate in the rocks[156]. Natural carbon uptake in thermodynamically stable carbonate minerals has now been recognized as a potential mechanism of permanently removing CO_2 from the atmosphere[164] and could help stabilize atmospheric greenhouse gas concentrations.

Timescales on which such hydrothermal fluids circulate through the oceanic lithosphere remain poorly constrained for most MOR environments, which has limited the understanding of

geochemical processes that depend on time. The short-lived radionuclide ^{223}Ra (half-life = 11 days) is abundant in Lost City fluids and has been used to constrain subsurface fluid residence times to less than 0.5–2 years[165]. These timescales are surprisingly similar to estimates from seafloor vents in volcanic-hosted systems[166,167] and are likely short enough to allow complex organic molecules to be exported into the overlying water column before they are destroyed. Short residence times also have important implications for understanding hydrothermal carbon transformation reactions that could have led to the formation of the first biomolecules and possibly early life on Earth[168].

[H2] *CH_4 formation*

Processes leading to reduced carbon species in marine hydrothermal systems and the role of serpentinization in CH_4 formation have become controversial[84,169,170]. Methane in peridotite-hosted systems (BOX 2) has long been attributed to abiotic Fischer-Tropsch or Sabatier reactions in ultramafic rocks[156,171], where hydration of olivine during serpentinization produces highly reducing conditions and H_2, leading to abiotic reduction of CO_2 to CH_4. Based on studies of fluid inclusions in SWIR gabbros[172,173], field and clumped isotope studies in the past decade suggest that gabbroic intrusions are also a potential source of CH_4 in hydrothermal systems[84,174,175]. Such studies postulate that CH_4 possibly forms in olivine-rich rocks early in the system when temperatures are hotter, is stored as fluid inclusions[84,169], and then is stripped from the rocks into modern fluids during hydrothermal circulation. The origin and the importance of CH_4 for microbial life on Earth and other planets are an active area of research and the processes of CH_4 production in marine ultramafic settings remain disputed[169,170].

Continued investigations of hydrothermal systems along the MAR and SWIR emphasise the importance of discontinuous magmatism and faulting that result in asymmetric ridge segments, exposure of gabbroic and ultramafic rocks, and marked differences in hydrothermal vent systems at slow-spreading ridges. In contrast to high temperature systems, Lost City-type systems are devoid of magmatic activity and driven by serpentinization processes.

[H1] Microbial diversity at hydrothermal vents

In this section, the marked differences in microbial communities between volcanic-hosted and peridotite-hosted hydrothermal systems[93,122,176] are discussed. Magma-driven systems support a high diversity of Bacteria and Archaea due to pronounced physical, thermal and chemical gradients that support a wide range of habitats (Fig. 4). In contrast, low-temperature, serpentinite-influenced systems devoid of magmatic activity, such as Lost City, support a low diversity of microorganisms (and macrofauna) and are dominated by CH_4-metabolizing archaea[177–179].

[H2] Diversity at magma-driven vents

Temperature and degree of seawater mixing between seawater and hydrothermal fluids are important determinants of high microbial diversity at magma-driven vents, as these factors affect the availability of electron acceptors and donors, and thus the energy-yielding microbial metabolisms[96] (FIG. 4). Different groups of vent-associated Bacteria and Archaea have been shown to grow over the temperature range of 2°C, in surrounding seawater and hydrothermal vent plumes[96], to at least 122°C in hot subsurface fluids[11,12,93].

[H3] Energy sources and redox reactions

In general, above 40°–60°C, oxygen is limiting such that the majority of microorganisms are anaerobic, using elemental sulphur, sulphate, nitrate and CO_2 as electron acceptors (FIG. 4a). CO_2 is the predominant source of carbon for all thermal groups of vent Bacteria and Archaea, although heterotrophs **[G]** have also been detected, even among some of the thermophilic archaea. In addition to sulphur, high levels of H_2 serve as the energy source for phylogenetically and physiologically diverse groups of Bacteria and Archaea. H_2-utilizing microorganisms have been identified in subsurface, black smoker and vent plume environments, and as animal symbionts[180]. H_2-utilizing proteobacteria dominate the cooler environments, whereas archaeal methanogens dominate the most extreme of the high temperature environments. The latter are limited in the availability of reduced or oxidized nitrogen sources, but hyperthermophilic **[G]** methanogens have been isolated that fix N_2[181]. Abiotic reactions that can reduce N_2 have also been identified under both volcanic-hosted and peridotite-hosted hydrothermal conditions[182,183]. Whether these reactions provide a source of reduced N for vent microorganisms is unknown.

Porous vent environments influenced by mixing with seawater – varying from subsurface habitats to black smoker chimney structures, and hydrothermal vent plumes advecting through the water column – support a markedly high diversity of Bacteria, including aerobes that utilize seawater-derived electron acceptors such as oxygen, sulphur, CO_2, nitrate, nitrite and nitrous oxide, and various metals including iron[42,96,184,185] (FIG. 4). Many members of vent bacteria derive energy from redox reactions involving electron acceptors such as nitrate and iron coupled to the oxidation of reduced sulfur compounds and H_2[184,186,187]. The dominant Archaea isolated from magma-driven vent environments include species from both the Euryarchaeota and the Crenarchaeota. Methanogens are dominant among Euryarchaeota, although Euryarchaeota also include many of the commonly isolated heterotrophic hyperthermophilic (75 to >100°C) Archaea,

some of which were among the first hyperthermophilic species isolated from hydrothermal vent environments in the 1980s.

[H3] Hydrothermal plumes and diffuse fluids

High temperature hydrothermal vents produce buoyant plumes that harbour a wide range of chemosynthetic microorganisms capable of oxidizing S, H_2, CH_4, Fe and Mn as energy sources and using CO_2 as the carbon source (FIG. 4b). The source of plume microorganisms is the deep ocean where they are ubiquitous. Active plume microbial communities comprise a substantial fraction of the deep ocean carbon pool, estimated to be comparable to the particulate organic carbon flux exported from pelagic sources[188].

Low temperature diffuse fluids at different vents within the same hydrothermal field indicate that individual diffuse flow sites can maintain unique microbial populations over time and have spatially distinct taxonomic, metabolic potential, and genetic characteristics[91,92,94]. The ability of an individual site to maintain an active subseafloor population is intrinsically linked to the geochemistry of the system, mixing conditions, and the geological characteristics of the individual vent site[92,176].

Microbial ecology has been revolutionized by new bioinformatics methods that use genome sequences to identify uncultivated microorganisms and viruses, which provide insight into their physiology and evolutionary history and help advance culturing techniques. Bioinformatic approaches have resulted in discoveries that not only have identified very high diversity of microorganisms in hydrothermal vent and subseafloor environments and the role of viruses in shaping that diversity, but also have profoundly changed the understanding of the evolutionary history of the microbial world[189]. A key discovery was the identification of the Lokiarchaeota in deep-sea sediments in the Arctic that had episodic hydrothermal input, likely

from the nearby basalt-hosted hydrothermal vents at Loki's Castle[190]. Lokiarchaeota share many characteristics previously thought to be found only in Eukaryotes, thus promising a better understanding of the evolution of eukaryotes[14,190,191] and supporting evidence for placing the Eukaryotes as emerging from the archaeal branch of the tree of life[192,193].

[H3] Growth rates of hydrothermal vent microorganisms

Most information on growth rates of vent microorganisms comes from laboratory studies of pure cultures and can vary with doubling times from minutes to hours. One of the major gaps in understanding the microbial ecology of vent environments is determining *in situ* growth rates and productivity of microbial communities. Determining *in situ* growth rates and productivity is a difficult task, particularly in diffuse fluids, because of mixing of different physiological groups of microorganisms from different depths that have marked gradients in temperature, electron acceptors and energy sources. An attempt to circumvent these obstacles involved the incubation of vent water samples from the EPR 9°50'N at *in situ* temperature and pressure with and without supplements of electron acceptors[194]. Microbial growth and carbon fixation rates were measured using subsurface water incubated at *in situ* temperature of 24°C and 50°C with and without O_2, NO_3^- and H_2. The results showed a production rate as high as those found in animal symbiosis and with doubling times of 17-41 hours. The authors identified three genera of the Campylobacteria group that included S and H_2 oxidizers as the dominant microbes. Campylobacteria are common in vent environments and represent 85% of the biomass in sulfide chimneys. Campylobacteria have also been identified as the dominant group in diffuse flow vents and in the shallow subseafloor[96]. While this study was limited to just one group of the diverse

608 population in vent fluids, it emphasizes that something must limit the accumulation of microbial
609 biomass given the rapid growth rates.
610 One possible limit to growth could be the widespread diversity of viruses including both
611 free-living and lysogenic (associated with the host genome) that are present in specific vent
612 environments[195]. The rate of virus lysis of vent microbes or the rate and specific genes
613 transferred by virus to bacteria is unknown. Moreover, there is evidence of protist grazing of
614 vent bacteria that appears to be particularly substantial in diffuse flow vent environments and
615 based on bacterial productivity rates[194], protists grazing could account for up to 22% of
616 chemosynthetic populations[196].
617
618 ***[H2] Diversity at serpentinite-hosted vents***
619 The microbial ecology of marine serpentinite-dominated vent environments is known
620 largely from Lost City. Less information is available from the more recently discovered site Old
621 City vent field at the SWIR[81] or from Logatchev and Rainbow. Early microbiology studies at Lost
622 City showed a very low diversity of microorganisms, with CH_4-metabolizing archaea dominating
623 at active, moderate temperature, anaerobic carbonate chimneys, and sulphur-metabolizing
624 Proteobacteria occupying the lower temperature, oxic or anoxic chimney environments[65,179,197]
625 (FIG. 4c). The CH_4-metabolizing archaea, which are related to the Methanosarcinales, exist as
626 complex biofilms within young, active carbonate chimneys. As the chimneys age and
627 hydrothermal input decreases, the dominance by Methanosarcinales shifts to complete
628 dominance by anaerobic CH_4-oxidizing archaea (ANME 1)[198]. Rare microbial taxa in the youngest
629 samples are progressively more dominant in older samples, suggesting that the Lost City

630 microbial community and perhaps other similar serpentinization environments are preadapted
631 to reoccurring environmental changes as an example of long-term ocean memory[199].
632 Molecular (DNA-based) characterization of the Lost City Methanosarcinales biofilm has
633 shown their potential to fix N_2, and based on an extraordinary abundance of transposable
634 elements, a potential for a very high incidence of gene transfer[200,201]. In laboratory experiments,
635 this biofilm has both produced and anaerobically oxidized CH_4, enhanced by H_2[201]. Low
636 concentrations of CO_2 in Lost City fluids indicates that these Methanosarcinales might utilize
637 alternate sources of carbon for CH_4 production, such as formate or acetate[157] (FIG. 4c). The
638 observation that sulphate-reducing bacteria convert formate to CO_2[177] has led to the hypothesis
639 that this CO_2 is then converted to CH_4[178]. The Lost City Methanosarcinales biofilm show multiple
640 morphologies, including cells with stacked, intracellular membranes similar to morphologies of
641 aerobic **[G]** methane-oxidizing bacteria, and might thus have some cells that oxidize methane
642 anaerobically[201]. Many questions remain about the Lost City microbial community, particularly
643 regarding Methanosarcinales, including their in-situ growth and activity rates, their diversity in
644 physiologies and potential syntrophic interactions.
645 Summarizing, magma-hosted hydrothermal systems host a vast, hot and diverse microbial
646 biosphere that sustain thriving macrofaunal communities at vents and contributes a substantial
647 fraction of the deep ocean carbon pool. In contrast, high pH serpentinizing hydrothermal systems
648 harbour distinctly more limited microbial communities dominated by methane- metabolizing
649 archaea.
650

[H1] Global fluxes and biogeochemical cycles

Hydrothermal circulation at MORs and ridge flanks controls global heat fluxes and plays an important role in regulating seawater chemistry, biogeochemical cycles, and input fluxes into subduction zones[87,202]. Although rates and directions of chemical exchange vary, hydrothermal processes are an important sink for seawater Mg, sulphate, and P and a source of volatiles and many elements, such as Fe and Mn and other metals[203], that serve as energy sources for microbial ecosystems at and beneath the seafloor.

[H2] Heat Flux

Most estimates of hydrothermal chemical fluxes combine convective heat output with compositional differences between hydrothermal fluids and seawater. A problem with this approach is to properly apportion heat flow between on-axis and ridge-flank regions. Current estimates put this distribution at 1.8 ± 0.3 TW and 8.1 ± 2 TW[7], respectively. Other estimates of heat flux use magma input, which lead to an average value of 50 MW km^{-1} (~3 TW) for the entire ridge system[204] or combine hydrothermal fluid concentrations with the compositions of the rocks in the subsurface[205], both of which tend to be lower than those using heat flux. However, vent fluid compositions can change dramatically with time, particularly following magmatic and seismic events[108,110], and we do not yet have an adequate understanding of the role played by these events relative to the steady-state flux.

[H2] Magnesium and calcium

The long standing Mg problem, which recognized that the riverine input of Mg was much larger than the known sinks[206], was notably improved by the discovery of Mg uptake in hydrothermal systems[207]. It is estimated that high temperature vent systems take up ~37% of the riverine Mg input and that low temperature alteration on ridge flanks accounts for another

674 ~14%[6]. Modern dolomite formation might account for a major fraction of the remaining Mg sink,
675 as indicated by Mg isotopes[208]. Although hydrothermal processes are both a sink and source of
676 Ca, the net flux of Ca is to the oceans[203] and is ~20% of riverine input[6]. An extensive list of
677 elements and compounds is found in REF[203].

678 ***[H2] Organic carbon***

679 Hydrothermal systems contribute to global carbon budgets by providing a notable fraction
680 of organic carbon to the deep ocean through microbial activity and oxidation of organic
681 compounds[188]. Heterotrophic microbial production rates are estimated to be up to 0.9 $gCm^{-2}yr^{-1}$
682 and could contribute 0.05 $GtCyr^{-1}$ of the particulate organic carbon (POC) within hydrothermal
683 plumes, similar to POC export fluxes of ~3 gCm^{-2} y^{-1} estimated for the deep Atlantic and Pacific
684 oceans[188]. Hydrothermal processes also influence the composition and fluxes of dissolved
685 organic carbon (DOC) to the ocean[209]. A large fraction of the deep ocean DOC is refractory[210] and
686 ranges from 4000 years old in the North Atlantic to 6000 years in the North Pacific[211]. High
687 temperature hydrothermal circulation alters and largely destroys DOC; however, diffuse vent
688 fluids contain higher DOC than deep seawater, which has been attributed to subsurface microbial
689 communities[212,213]. Ridge flank fluids contain less DOC than deep seawater and can be as old as
690 17,000 years[212,214,215]. DOC older than deep North Atlantic water was also found emanating from
691 cold oceanic crust at North Pond near the MAR[216]. These data coupled with findings of 6900-
692 year-old DOC near the East Pacific Rise at 25°S[217] have led to the speculation that hydrothermal
693 venting could be an important source of old DOC to the deep ocean[209].

694 Hydrothermal circulation can also lead to the incorporation of DOC in basement rocks;
695 total organic carbon could be up to ~1500 ppm in oceanic ultramafic and up to ~600 ppm in
696 gabbroic rocks[218,219]. Stable isotope and radiocarbon studies of the Atlantis Massif[163] indicate

that organic carbon with an average radiocarbon age of 14,000 years is incorporated during serpentinization and suggest that oxidation of organic compounds along circulation paths could provide carbon for carbonates. REF[163] estimated annual storage rates of up to 1.7×10^{11} mol C yr^{-1} of organic carbon and up to 6×10^{12} mol C yr^{-1} of inorganic carbon in serpentinized oceanic peridotites.

[H2] Iron

Hydrothermal Fe fluxes to the deep ocean and the impact they could have on primary productivity and nitrogen fixation are currently an exciting area of research. Early studies had assumed that Fe from high temperature systems would quickly precipitate out of the plumes as sulphide or oxygenated particles. However, Fe can be transported thousands of kilometres across ocean basins away from the hydrothermal source either as nanoparticles or as organically chelated dissolved iron[220]. Current estimates of dissolved Fe flux are 4-6 x 10^{9} mole yr^{-1}, REFS[220,221]. This flux is thought to be a notable source to the deep ocean that could eventually upwell and promote primary production in the so-called High Nitrate Low Chlorophyll (HTLC) regions where Fe is considered to be the limiting nutrient. The Southern Ocean is one of these important HTLC regions, where Fe is thought to lead to phytoplankton blooms[222,223]. Modelling has shown that upwelling of hydrothermal Fe might be responsible for 15-30% of the primary production in this region, thus linking the global biogeochemical cycles of iron and carbon. Fe from shallow hydrothermal plumes **[G]** at the Tonga-Kermadec Arc is an important component of increased nitrogen fixation and primary production in that region[224,225].

There is currently extensive research on the topic of Fe fluxes and much to be learned regarding the importance of hydrothermal sources of Fe and other trace metals to the deep ocean. To date, most hydrothermal chemical flux estimates are based on basalt-hosted MOR

systems. However, it is well accepted that hydrothermal circulation at all ridges and ridge flanks contributes to global heat fluxes and has an important role in regulating seawater chemistry, the composition of the oceanic crust and biogeochemical cycles. Release of many hydrothermally-related compounds to the water-column has an immediate effect on chemoorganotrophic activity within hydrothermal plumes, representing a substantial organic carbon export flux in the deep ocean[188]. A full understanding of hydrothermal fluxes requires further research of back-arc spreading centres, island-arc and peridotite-hosted sites as well as tackling the difficult job of quantifying temporal variability in vent fluids[40,108].

[H1] Summary and future perspectives

The theories of plate tectonics and seafloor-spreading revolutionized Earth and ocean sciences and paved the way for new oceanographic, analytical and theoretical approaches to understand how Earth works. However, fundamental gaps remain in understanding the interplay among geological and biogeochemical processes and in quantifying the hydrogeology of hydrothermal systems and the impact of fluid pathways at ridges and ridge flanks on heat, chemical, and biological fluxes to the ocean.

The discovery of submarine hydrothermal vents supporting chemosynthetic communities led to revolutionary understanding of the tree of life[190] and the conditions under which life can thrive, survive, and die. Indeed, we are beginning to acquire a glimpse of the rare deep biosphere within the lithosphere and hydrothermal vents[95] and have started to make progress towards understanding the importance of viruses[195] and fungi[226] in these systems. However, little is known about how organisms and viruses evolve over time, how these communities interact, and to what extent vents are sources for organisms in the overlying ocean.

743 Advanced sampling, spectroscopic and chromatographic techniques have also started to
744 unravel the compositions, sources and decomposition of DOC and complex organic compounds
745 in hydrothermal systems[227–230]. The continued development of compound specific radiocarbon
746 analyses and new sampling and analytical techniques are needed to further understand the
747 composition, age and fate of seawater and hydrothermally derived DOC and its potential
748 contribution to deep ocean DOC.
749 Technical innovation and installation of ocean observatories have advanced the ability for
750 monitoring and allows for rapid response to magmatic and tectonic activity, providing real-time
751 information on the development of diking-eruptive events from their inception (BOX 1).
752 Advancing these capabilities is vital for future research and will require more sophisticated
753 sensors, cabled and uncabled instrument networks and advanced underwater vehicles[231,232].
754 Future research will be guided by advances in robotic technologies together with miniaturization
755 and automation of sensor systems[233]. Development of in-situ chemical, physical and
756 metagenomic sensors for long-term deployments on the seafloor and in the overlying water
757 column will allow the detection of ephemeral processes that have been missed by traditional
758 oceanographic methods and will provide information on how these systems evolve over time.
759 Understanding the processes that control the dynamic interplay of geology, chemistry and
760 biology within the oceans and rocks beneath it will become increasingly important as humans
761 continue to influence the Earth's oceans and atmosphere. Continued exploration of
762 hydrothermal environments promises to offer new insights across multiple disciplines. It is vital
763 that these systems are not exploited in ways that could destroy or irreversibly alter them, which
764 would result in lost opportunities for new discoveries and limit future insight into the processes

765 that shape the planet. The deep sea holds many spectacular wonders, with many more to
766 discover – and much to protect.
767
768 **References**

769 1. Parsons, B. The rates of plate creation and consumption. *Geophysical Journal*
770 *International* **67**, 437–448 (1981).
771 2. Sinha, M. C. & Evans, R. L. Gephysical Constraints upon the Thermal Regime of the
772 Ocean Crust. in *Geophysical Monograph Series 148* (eds. German, C. R., Lin, J. &
773 Parson, L. M.) 19–62 (American Geophysical Union, 2004). doi:10.1029/148GM02.
774 3. German, C. R. & Lin, J. The thermal structure of the oceanic crust, ridge-spreading
775 and hydrothermal circulation: How well do we understand their inter-connections? in
776 *Geophysical Monograph Series* (eds. German, C. R., Lin, J. & Parson, L. M.) 1–18
777 (American Geophysical Union, 2004). doi:10.1029/148GM01.
778 4. Wheat, C. G., Fisher, A. T., McManus, J., Hulme, S. M. & Orcutt, B. N. Cool seafloor
779 hydrothermal springs reveal global geochemical fluxes. *Earth and Planetary Science*
780 *Letters* **476**, 179–188 (2017).
781 5. Stein, C. A. & Stein, S. Constraints on hydrothermal heat flux through the oceanic
782 lithosphere from global heat flow. *J. Geophys. Res.* **99**, 3081–3095 (1994).
783 6. Mottl, M. Partitioning of energy and mass fluxes between mid-ocean ridge axes and
784 flanks at high and low temperature. in *Energy and Mass Transfer in Submarine*
785 *Hydrothermal Systems, P. Halbach, V. Tunnicliffe, J. Hein (Eds.)* 271–286 (Dahlem
786 University Press, 2003).

7. Wheat, C.G. & Mottl, M.J. Geochemical fluxes through mid-ocean ridge flanks. in *Hydrogeology of the Oceanic Lithosphere* 627–658 (Cambridge University Press, 2004).
8. Cavanaugh, C. M., Gardiner, S. L., Jones, M. L., Jannasch, H. W. & Waterbury, J. B. Prokaryotic cells in the hydrothermal vent tube worm *Riftia pachyptila* Jones: Possible chemoautotrophic symbionts. *Science* **213**, 340–342 (1981).
9. Lilley, M. D., Baross, J. A. & Gordon, L. I. Reduced Gases and Bacteria in Hydrothermal Fluids: The Galapagos Spreading Center and 21°N East Pacific Rise. in *Hydrothermal Processes at Seafloor Spreading Centers* (eds. Rona, P. A., Boström, K., Laubier, L. & Smith, K. L.) 411–449 (Springer US, 1983). doi:10.1007/978-1-4899-0402-7_18.
10. Corliss, J. B. *et al.* Submarine Thermal Springs on the Galápagos Rift. *Science* **203**, 1073–1083 (1979).
11. Takai, K. *et al.* Cell proliferation at 122°C and isotopically heavy CH4 production by a hyperthermophilic methanogen under high-pressure cultivation. *Proc. Natl. Acad. Sci. USA* **105**, 10949–10954 (2008).
12. Kashefi, K. & Lovley, D. R. Extending the upper temperature limit for life. *Science* **301**, 934–934 (2003).
13. Weiss, M. C. *et al.* The physiology and habitat of the last universal common ancestor. *Nat Microbiol* **1**, 16116 (2016).
14. Spang, A. & Ettema, T. J. G. Microbial diversity: The tree of life comes of age. *Nat Microbiol* **1**, 16056 (2016).
15. Spiess, F. N. *et al.* East Pacific Rise: Hot Springs and Geophysical Experiments. *Science* **207**, 1421–1433 (1980).

16. Von Damm, K. L. *et al.* Chemistry of submarine hydrothermal solutions at 21 °N, East Pacific Rise. *Geochimica et Cosmochimica Acta* **49**, 2197–2220 (1985).
17. Felbeck, H. Chemoautotrophic Potential of the Hydrothermal Vent Tube Worm, *Riftia pachyptila* Jones (Vestimentifera). *Science* **213**, 336–338 (1981).
18. Beaulieu, S. E., Baker, E. T., German, C. R. & Maffei, A. An authoritative global database for active submarine hydrothermal vent fields. *Geochem. Geophys. Geosyst.* **14**, 4892–4905 (2013).
19. Jannasch, H. W. & Wirsen, C. O. Chemosynthetic Primary Production at East Pacific Sea Floor Spreading Centers. *BioScience* **29**, 592–598 (1979).
20. Hey, R. *et al.* Tectonic/volcanic segmentation and controls on hydrothermal venting along Earth's fastest seafloor spreading system, EPR 27°-32°S: Segmentation along the EPR. *Geochem. Geophys. Geosyst.* **5**, (2004).
21. Carbotte, S. & Macdonald, K. East Pacific Rise 8°–10°30′N: Evolution of ridge segments and discontinuities from SeaMARC II and three-dimensional magnetic studies. *J. Geophys. Res.* **97**, 6959 (1992).
22. Anonymous. Penrose field conference on ophiolites. *Geotimes* **17**, 24–25 (1972).
23. Carbotte, S. M. *et al.* Stacked magma lenses beneath mid- ocean ridges: Insights from new seismic observations and synthesis with prior geophysical and geologic findings. *J Geophys Res Solid Earth* **126**, 10.1029/2020JB021434 (2021).
24. Sinton, J. M. & Detrick, R. S. Mid-ocean ridge magma chambers. *J. Geophys. Res.* **97**, 197–216 (1992).
25. Coogan, L. A. The Lower Oceanic Crust. in *Treatise on Geochemistry* 497–541 (Elsevier, 2014). doi:10.1016/B978-0-08-095975-7.00316-8.

26. Brown, T. C. *et al.* Textural Character of Gabbroic Rocks from Pito Deep: a Record of Magmatic Processes and the Genesis of the Upper Plutonic Crust at Fast-Spreading Mid-Ocean Ridges. *Journal of Petrology* **60**, 997–1026 (2019).
27. Maher, S. M., Gee, J. S., Cheadle, M. J. & John, B. E. Three-dimensional magnetic stripes require slow cooling in fast-spread lower ocean crust. *Nature* **597**, 511–515 (2021).
28. Karson, J. A., Kelley, D. S., Fornari, D. J., Perfit, M. R. & Shank, T. M. *Discovering the Deep: A Photographic Atlas of the Seafloor and Ocean Crust*. (Cambridge University Press, 2015). doi:10.1017/CBO9781139050524.
29. Haymon, R. M. *et al.* Volcanic eruption of the mid-ocean ridge along the East Pacific Rise crest at 9°45–52′N: Direct submersible observations of seafloor phenomena associated with an eruption event in April, 1991. *Earth and Planetary Science Letters* **119**, 85–101 (1993).
30. Von Damm, K. L. *et al.* Evolution of East Pacific Rise hydrothermal vent fluids following a volcanic eruption. *Nature* **375**, 47–50 (1995).
31. Von Damm, K. L. Controls on the Chemistry and Temporal Variability of Seafloor Hydrothermal Fluids. in *Geophysical Monograph Series* (eds. Humphris, S. E., Zierenberg, R. A., Mullineaux, L. S. & Thomson, R. E.) 222–247 (American Geophysical Union, 1995). doi:10.1029/GM091p0222.
32. Tolstoy, M. *et al.* A Sea-Floor Spreading Event Captured by Seismometers. *Science* **314**, 1920–1922 (2006).
33. Tan, Y. J., Tolstoy, M., Waldhauser, F. & Wilcock, W. S. D. Dynamics of a seafloor-spreading episode at the East Pacific Rise. *Nature* **540**, 261–265 (2016).

34. Tolstoy, M., Waldhauser, F., Bohnenstiehl, D. R., Weekly, R. T. & Kim, W.-Y. Seismic identification of along-axis hydrothermal flow on the East Pacific Rise. *Nature* **451**, 181–184 (2008).
35. Delaney, J. R. *et al.* The quantum event of oceanic crustal accretion: Impacts of diking at mid-ocean ridges. *Science* **281**, 222–230 (1998).
36. Baker, E. T. *et al.* Posteruption enhancement of hydrothermal activity: A 33- Year, multieruption time series at Axial Seamount (Juan de Fuca Ridge). *Geochem. Geophys. Geosyst.* **20**, 814–828 (2019).
37. Clague, D. A. *et al.* Geologic history of the summit of Axial Seamount, Juan de Fuca Ridge: Geologic History of Axial Seamount. *Geochem. Geophys. Geosyst.* **14**, 4403–4443 (2013).
38. Chadwick, W. W., Nooner, S. L., Butterfield, D. A. & Lilley, M. D. Seafloor deformation and forecasts of the April 2011 eruption at Axial Seamount. *Nature Geosci* **5**, 474–477 (2012).
39. Wilcock, W. S. D. Physical response of mid-ocean ridge hydrothermal systems to local earthquakes. *Geochem. Geophys. Geosyst.* **5**, 10.1029/2004GC000701 (2004).
40. Lilley, M. D., Butterfield, D. A., Lupton, J. E. & Olson, E. J. Magmatic events can produce rapid changes in hydrothermal vent chemistry. *Nature* **422**, 878–881 (2003).
41. Delaney, J. R., Robigou, V., McDuff, R. E. & Tivey, M. K. Geology of a vigorous hydrothermal system on the Endeavour Segment, Juan de Fuca Ridge. *J. Geophys. Res.* **97**, 19663–19682 (1992).
42. Kelley, D. S., Baross, J. A. & Delaney, J. R. Volcanoes, Fluids, and Life at Mid-Ocean Ridge Spreading Centers. *Annu. Rev. Earth Planet. Sci.* **30**, 385–491 (2002).

43. Kelley, D. *et al.* Endeavour Segment of the Juan de Fuca Ridge: One of the Most Remarkable Places on Earth. *oceanog* **25**, 44–61 (2012).
44. Clague, D. A. *et al.* Hydrothermal Chimney Distribution on the Endeavour Segment, Juan de Fuca Ridge. *Geochem. Geophys. Geosyst.* **21**, (2020).
45. Robigou, V., Delaney, J. R. & Stakes, D. S. Large massive sulfide deposits in a newly discovered active hydrothermal system, The High-Rise Field, Endeavour Segment, Juan De Fuca Ridge. *Geophys. Res. Lett.* **20**, 1887–1890 (1993).
46. Bird, P. An updated digital model of plate boundaries: *Geochem. Geophys. Geosyst.* **4**, (2003).
47. Cannat, M., Fontaine, F. & Escartín, J. Serpentinization and associated hydrogen and methane fluxes at slow spreading ridges. in *Geophysical Monograph Series* (eds. Rona, P. A., Devey, C. W., Dyment, J. & Murton, B. J.) vol. 188 241–264 (American Geophysical Union, 2010).
48. John, B. E. & Cheadle, M. J. Deformation and alteration associated with oceanic and continental detachment fault systems: Are they similar? in *Geophysical Monograph Series* (eds. Rona, P. A., Devey, C. W., Dyment, J. & Murton, B. J.) vol. 188 175–205 (American Geophysical Union, 2010).
49. Escartín, J. *et al.* Central role of detachment faults in accretion of slow-spreading oceanic lithosphere. *Nature* **455**, 790–794 (2008).
50. Cannat, M. *et al.* Thin crust, ultramafic exposures, and rugged faulting patterns at the Mid-Atlantic Ridge (22°–24°N). *Geol* **23**, 49 (1995).
51. Tucholke, B. E., Lin, J. & Kleinrock, M. C. Megamullions and mullion structure defining oceanic metamorphic core complexes on the Mid-Atlantic Ridge. *J. Geophys. Res.* **103**, 9857–9866 (1998).

52. Karson, J. A. Internal Structure of Oceanic Lithosphere: A Perspective from Tectonic Windows. in *Geophysical Monograph Series* (eds. Roger Buck, W., Delaney, P. T., Karson, J. A. & Lagabrielle, Y.) vol. 106 177–218 (American Geophysical Union, 1998).
53. Cannat, M. *et al.* Spreading rate, spreading obliquity, and melt supply at the ultraslow spreading Southwest Indian Ridge. *Geochem. Geophys. Geosyst.* **9**, 10.1029/2007GC001676 (2008).
54. Escartín, J. *et al.* Tectonic structure, evolution, and the nature of oceanic core complexes and their detachment fault zones (13°20′N and 13°30′N, Mid Atlantic Ridge). *Geochem. Geophys. Geosyst.* **18**, 1451–1482 (2017).
55. Smith, D. K., Escartín, J., Schouten, H. & Cann, J. R. Fault rotation and core complex formation: Significant processes in seafloor formation at slow-spreading mid-ocean ridges (Mid-Atlantic Ridge, 13°-15°N). *Geochem. Geophys. Geosyst.* **9**, (2008).
56. Cannat, M. *et al.* Modes of seafloor generation at a melt-poor ultraslow-spreading ridge. *Geol* **34**, 605–608 (2006).
57. Dick, H. J. B., Tivey, M. A. & Tucholke, B. E. Plutonic foundation of a slow-spreading ridge segment: Oceanic core complex at Kane Megamullion, 23°30′N, 45°20′W. *Geochem. Geophys. Geosyst.* **9**, (2008).
58. Sauter, D. *et al.* Continuous exhumation of mantle-derived rocks at the Southwest Indian Ridge for 11 million years. *Nature Geosci* **6**, 314–320 (2013).
59. Michael, P. J. *et al.* Magmatic and amagmatic seafloor generation at the ultraslow-spreading Gakkel ridge, Arctic Ocean. *Nature* **423**, 956–961 (2003).
60. MacLeod, C. J. *et al.* Life cycle of oceanic core complexes. *Earth and Planetary Science Letters* **287**, 333–344 (2009).

61. Schroeder, T. & John, B. E. Strain localization on an oceanic detachment fault system, Atlantis Massif, 30°N, Mid-Atlantic Ridge. *Geochem. Geophys. Geosyst.* **5**, 10.1029/2004GC000728 (2004).
62. Bickert, M., Lavier, L. & Cannat, M. How do detachment faults form at ultraslow mid-ocean ridges in a thick axial lithosphere? *Earth and Planetary Science Letters* **533**, 116048 (2020).
63. McCaig, A. M., Delacour, A., Fallick, A. E., Castelain, T. & Früh-Green, G. L. Detachment fault control on hydrothermal circulation systems: Interpreting the subsurface beneath the TAG hydrothermal field using the isotopic and geological evolution of oceanic core complexes in the Atlantic. in *Geophysical Monograph Series* (eds. Rona, P. A., Devey, C. W., Dyment, J. & Murton, B. J.) vol. 188 207–239 (American Geophysical Union, 2010).
64. Boschi, C., Früh-Green, G. L., Delacour, A., Karson, J. A. & Kelley, D. S. Mass transfer and fluid flow during detachment faulting and development of an oceanic core complex, Atlantis Massif (MAR 30°N). *Geochem. Geophys. Geosyst.* **7**, doi:10.1029/2005GC001074. (2006).
65. Kelley, D. S. *et al.* A Serpentinite-Hosted Ecosystem: The Lost City Hydrothermal Field. *Science* **307**, 1428–1434 (2005).
66. Karson, J. A. *et al.* Detachment shear zone of the Atlantis Massif core complex, Mid-Atlantic Ridge, 30°N. *Geochem. Geophys. Geosyst.* **7**, (2006).
67. Colaço, A. *et al.* MoMAR-D: a technological challenge to monitor the dynamics of the Lucky Strike vent ecosystem. *ICES Journal of Marine Science* **68**, 416–424 (2011).

68. Barreyre, T. *et al.* Structure, temporal evolution, and heat flux estimates from the Lucky Strike deep-sea hydrothermal field derived from seafloor image mosaics. *Geochem. Geophys. Geosyst.* **13**, 10.1029/2011GC003990 (2012).
69. Mittelstaedt, E. *et al.* Quantifying diffuse and discrete venting at the Tour Eiffel vent site, Lucky Strike hydrothermal field. *Geochem. Geophys. Geosyst.* **13**, 10.1029/2011GC003991 (2012).
70. Lowell, R. P. *et al.* Magma-hydrothermal interactions at the Costa Rica Rift from data collected in 1994 and 2015. *Earth and Planetary Science Letters* **531**, 115991 (2020).
71. Fontaine, F. J., Cannat, M., Escartin, J. & Crawford, W. C. Along-axis hydrothermal flow at the axis of slow spreading Mid-Ocean Ridges: Insights from numerical models of the Lucky Strike vent field (MAR). *Geochem. Geophys. Geosyst.* **15**, 2918–2931 (2014).
72. McCaig, A. M., Cliff, R. A., Escartin, J., Fallick, A. E. & MacLeod, C. J. Oceanic detachment faults focus very large volumes of black smoker fluids. *Geol* **35**, 935–938 (2007).
73. Kent, G. M., Harding, A. J. & Orcutt, J. A. Distribution of magma beneath the East Pacific Rise between the Clipperton Transform and the 9°17′N Deval from forward modeling of common depth point data. *J. Geophys. Res.* **98**, 13945–13969 (1993).
74. Canales, J. P. *et al.* Upper crustal structure and axial topography at intermediate spreading ridges: Seismic constraints from the southern Juan de Fuca Ridge. *J. Geophys. Res.* **110**, B12104 (2005).
75. Phipps Morgan, J. & Chen, Y. J. Dependence of ridge-axis morphology on magma supply and spreading rate. *Nature* **364**, 706–708 (1993).

76. deMartin, B. J., Sohn, R. A., Pablo Canales, J. & Humphris, S. E. Kinematics and geometry of active detachment faulting beneath the Trans-Atlantic Geotraverse (TAG) hydrothermal field on the Mid-Atlantic Ridge. *Geol* **35**, 711–714 (2007).
77. Cannat, M. Emplacement of mantle rocks in the seafloor at mid-ocean ridges. *J. Geophys. Res.* **98**, 4163–4172 (1993).
78. Wilcock, W. S. D. & Delaney, J. R. Mid-ocean ridge sulfide deposits: Evidence for heat extraction from magma chambers or cracking fronts? *Earth and Planetary Science Letters* **145**, 49–64 (1996).
79. Kelley, D. S. & Shank, T. M. Hydrothermal systems: A decade of discovery in slow spreading environments. in *Geophysical Monograph Series* (eds. Rona, P. A., Devey, C. W., Dyment, J. & Murton, B. J.) vol. 188 369–407 (American Geophysical Union, 2010).
80. Kelley, D. S. *et al.* An off-axis hydrothermal vent field near the Mid-Atlantic Ridge at 30° N. *Nature* **412**, 145–149 (2001).
81. Lecoeuvre, A., Ménez, B., Cannat, M., Chavagnac, V. & Gérard, E. Microbial ecology of the newly discovered serpentinite-hosted Old City hydrothermal field (southwest Indian ridge). *ISME J* **15**, 818–832 (2021).
82. Connelly, D. P. *et al.* Hydrothermal vent fields and chemosynthetic biota on the world's deepest seafloor spreading centre. *Nat Commun* **3**, 620 (2012).
83. German, C. R. *et al.* Diverse styles of submarine venting on the ultraslow spreading Mid-Cayman Rise. *Proc. Natl. Acad. Sci. USA* **107**, 14020–14025 (2010).
84. McDermott, J. M., Seewald, J. S., German, C. R. & Sylva, S. P. Pathways for abiotic organic synthesis at submarine hydrothermal fields. *Proc Natl Acad Sci USA* **112**, 7668–7672 (2015).

85. Hayman, N. W. *et al.* Oceanic core complex development at the ultraslow spreading Mid-Cayman Spreading Center. *Geochem. Geophys. Geosyst.* **12**, 10.1029/2010GC003240 (2011).
86. Barreyre, T., Parnell- Turner, R., Wu, J. - N. & Fornari, D. J. Tracking Crustal Permeability and Hydrothermal Response During Seafloor Eruptions at the East Pacific Rise, 9°50'N. *Geophysical Research Letters* **49**, (2022).
87. Alt, J. C. Subseafloor Processes in Mid-Ocean Ridge Hydrothermal Systems. in *Seafloor Hydrothermal Systems: Physical, Chemical, Biological, and Geological Interactions* (eds. Humphris, S. E., Zierenberg, R. A., Mullineaux, L. S. & Thomson, R. E.) vol. 91 85–114 (American Geophysical Union, 1995).
88. Tivey, M. K. Generation of seafloor hydrothermal vent fluids and associated mineral deposits. *Oceanography* **20**, 50–65 (2007).
89. Butterfield, D. A. *et al.* Mixing, reaction and microbial activity in the sub-seafloor revealed by temporal and spatial variation in diffuse flow vents at Axial Volcano. in *Geophysical Monograph Series* (eds. Wilcock, W. S. D., DeLong, E. F., Kelley, D. S., Baross, J. A. & Craig Cary, S.) vol. 144 269–289 (American Geophysical Union, 2004).
90. Von Damm, K. L. & Lilley, M. D. Diffuse flow hydrothermal fluids from 9° 50′ N East Pacific Rise: Origin, evolution and biogeochemical controls. in *Geophysical Monograph Series* (eds. Wilcock, W. S. D., DeLong, E. F., Kelley, D. S., Baross, J. A. & Craig Cary, S.) vol. 144 245–268 (American Geophysical Union, 2004).
91. Opatkiewicz, A. D., Butterfield, D. A. & Baross, J. A. Individual hydrothermal vents at Axial Seamount harbor distinct subseafloor microbial communities. *FEMS Microbiology Ecology* **70**, 413–424 (2009).

92. Fortunato, C. S., Larson, B., Butterfield, D. A. & Huber, J. A. Spatially distinct, temporally stable microbial populations mediate biogeochemical cycling at and below the seafloor in hydrothermal vent fluids: Microbial genomics at axial seamount. *Environ Microbiol* **20**, 769–784 (2018).
93. Deming, J. W. & Baross, J. A. Deep-sea smokers: Windows to a subsurface biosphere? *Geochimica et Cosmochimica Acta* **57**, 3219–3230 (1993).
94. Huber, J. A. *et al.* Microbial Population Structures in the Deep Marine Biosphere. *Science* **318**, 97–100 (2007).
95. Sogin, M. L. *et al.* Microbial diversity in the deep sea and the underexplored “rare biosphere”. *Proc. Natl. Acad. Sci. USA* **103**, 12115–12120 (2006).
96. Dick, G. J. The microbiomes of deep-sea hydrothermal vents: distributed globally, shaped locally. *Nat Rev Microbiol* (2019) doi:10.1038/s41579-019-0160-2.
97. Bischoff, J. L. & Rosenbauer, R. J. An empirical equation of state for hydrothermal seawater (3.2 percent NaCl). *American Journal of Science* **285**, 725–763 (1985).
98. Kelley, D. S. & Delaney, J. R. Two-phase separation and fracturing in mid-ocean ridge gabbros at temperatures greater than 700°C. *Earth and Planetary Science Letters* **83**, 53–66 (1987).
99. Fournier, R. O. Conceptual models of brine evolution in magmatic-hydrothermal systems. *US Geol. Surv. Prof. Pap.* **1350**, 1487–1506 (1987).
100. Coumou, D., Driesner, T., Weis, P. & Heinrich, C. A. Phase separation, brine formation, and salinity variation at Black Smoker hydrothermal systems. *J. Geophys. Res.* **114**, B03212 (2009).
101. Chavagnac, V. *et al.* Spatial Variations in Vent Chemistry at the Lucky Strike Hydrothermal Field, Mid- Atlantic Ridge (37°N): Updates for subseafloor flow

geometry from the newly discovered Capelinhos Vent. *Geochem. Geophys. Geosyst.* **19**, 4444–4458 (2018).

102. Xu, G. & Lavelle, J. W. Circulation, hydrography, and transport over the summit of Axial seamount, a deep volcano in the Northeast Pacific. *J. Geophys. Res. Oceans* **122**, 5404–5422 (2017).

103. Kaye, J. Z. & Baross, J. A. High incidence of halotolerant bacteria in Pacific hydrothermal-vent and pelagic environments. *FEMS Microbiology Ecology* **32**, 249–260 (2000).

104. Haase, K. M. *et al.* Young volcanism and related hydrothermal activity at 5°S on the slow-spreading southern Mid-Atlantic Ridge. *Geochem. Geophys. Geosyst.* **8**, (2007).

105. Koschinsky, A. *et al.* Hydrothermal venting at pressure-temperature conditions above the critical point of seawater, 5°S on the Mid-Atlantic Ridge. *Geol* **36**, 615–618 (2008).

106. Pester, N. J., Ding, K. & Seyfried, W. E. Magmatic eruptions and iron volatility in deep-sea hydrothermal fluids. *Geology* **42**, 255–258 (2014).

107. Butterfield, D. A. *et al.* Seafloor eruptions and evolution of hydrothermal fluid chemistry. in *Mid-Ocean Ridges* (eds. Cann, J. R., Elderfield, H. & Laughton, A. S.) 153–170 (Cambridge University Press, 1999). doi:10.1017/CBO9780511600050.008.

108. Von Damm, K. L. Chemistry of hydrothermal vent fluids from 9°-10°N, East Pacific Rise: “Time zero,” the immediate posteruptive period. *J. Geophys. Res.* **105**, 11203–11222 (2000).

109. Von Damm, K. L. *et al.* Extraordinary phase separation and segregation in vent fluids from the southern East Pacific Rise. *Earth and Planetary Science Letters* **206**, 365–378 (2003).

110. Butterfield, D. A. *et al.* Seafloor eruptions and evolution of hydrothermal fluid chemistry. *Philosophical Transactions of the Royal Society of London. Series A: Mathematical, Physical and Engineering Sciences* **355**, 369–386 (1997).

111. Seewald, J., Cruse, A. & Saccocia, P. Aqueous volatiles in hydrothermal fluids from the Main Endeavour Field, northern Juan de Fuca Ridge: temporal variability following earthquake activity. *Earth and Planetary Science Letters* **216**, 575–590 (2003).

112. Love, B., Lilley, M., Butterfield, D., Olson, E. & Larson, B. Rapid variations in fluid chemistry constrain hydrothermal phase separation at the Main Endeavour Field. *Geochem. Geophys. Geosyst.* **18**, 531–543 (2017).

113. Rommevaux, C. *et al.* Prokaryote Communities at Active Chimney and *In Situ* Colonization Devices After a Magmatic Degassing Event (37°N MAR, EMSO- Azores Deep- Sea Observatory). *Geochem. Geophys. Geosyst.* **20**, 3065–3089 (2019).

114. Baker, E. T., Massoth, G. J. & Feely, R. A. Cataclysmic hydrothermal venting on the Juan de Fuca Ridge. *Nature* **329**, 149–151 (1987).

115. Lupton, J. E., Baker, E. T. & Massoth, G. J. Helium, heat, and the generation of hydrothermal event plumes at mid-ocean ridges. *Earth and Planetary Science Letters* **171**, 343–350 (1999).

116. Holden, J. F., Summit, M. & Baross, J. A. Thermophilic and hyperthermophilic microorganisms in 3–30°C hydrothermal fluids following a deep-sea volcanic eruption. *FEMS Microbiology Ecology* **25**, 33–41 (1998).

117. Summit, M. & Baross, J. A. Thermophilic subseafloor microorganisms from the 1996 North Gorda Ridge eruption. *Deep Sea Research Part II: Topical Studies in Oceanography* **45**, 2751–2766 (1998).

118. Kelley, D. S., Lilley, M. D., Lupton, J. E. & Olson, E. J. Enriched H2, CH4, and 3He concentrations in hydrothermal plumes associated with the 1996 Gorda Ridge eruptive event. *Deep Sea Research Part II: Topical Studies in Oceanography* **45**, 2665–2682 (1998).

119. Spietz, R. *et al.* Deep-Sea Volcanic Eruptions Create Unique Chemical and Biological Linkages Between the Subsurface Lithosphere and the Oceanic Hydrosphere. *Oceanog* **31**, 128–135 (2018).

120. Chadwick, W. W. *et al.* The 1998 eruption of Axial Seamount: New insights on submarine lava flow emplacement from high-resolution mapping. *Geochem. Geophys. Geosyst.* **14**, 3939–3968 (2013).

121. Gold, T. The deep, hot biosphere. *Proc. Natl. Acad. Sci. USA* **89**, 6045–6049 (1992).

122. Baross, J. A., Wilcock, W. S. D., Kelley, D. S., DeLong, E. F. & Craig Cary, S. The subsurface biosphere at Mid-Ocean Ridges: Issues and challenges. in *Geophysical Monograph Series* (eds. Wilcock, W. S. D., DeLong, E. F., Kelley, D. S., Baross, J. A. & Craig Cary, S.) vol. 144 1–11 (American Geophysical Union, 2004).

123. Davis, E. E. & Fisher, A. T. Heat Flow, Seafloor: Methods and Observations. in *Encyclopedia of Solid Earth Geophysics* (ed. Gupta, H. K.) 1–13 (Springer International Publishing, 2020). doi:10.1007/978-3-030-10475-7_65-1.

124. Simoneit, B. R. T., Kawka, O. E. & Brault, M. Origin of gases and condensates in the Guaymas Basin hydrothermal system (Gulf of California). *Chemical Geology* **71**, 169–182 (1988).

125. Cruse, A. M. & Seewald, J. S. Geochemistry of low-molecular weight hydrocarbons in hydrothermal fluids from Middle Valley, northern Juan de Fuca Ridge. *Geochimica et Cosmochimica Acta* **70**, 2073–2092 (2006).

126. Proceedings of the Ocean Drilling Program, 139 Scientific Results. **139**, (1994).

127. Zierenberg, R. A., Fouquet, Y., Miller, D. J. & Normark, W. R. Proceedings of the Ocean Drilling Program, Scientific Results, 169. http://www-odp.tamu.edu/publications/169_SR/169TOC.HTM (2000) doi:10.2973/odp.proc.sr.169.2000.

128. Ishibashi, J. *et al.* Helium and carbon gas geochemistry of pore fluids from the sediment-rich hydrothermal system in Escanaba Trough. *Applied Geochemistry* **17**, 1457–1466 (2002).

129. Von Damm, K. L. *et al.* The Escanaba Trough, Gorda Ridge hydrothermal system: Temporal stability and subseafloor complexity. *Geochimica et Cosmochimica Acta* **69**, 4971–4984 (2005).

130. Teske, A. *et al.* The Guaymas Basin Hiking Guide to Hydrothermal Mounds, Chimneys, and Microbial Mats: Complex Seafloor Expressions of Subsurface Hydrothermal Circulation. *Front. Microbiol.* **7**, 10.3389/fmicb.2016.00075 (2016).

131. Paduan, J. B. *et al.* Discovery of Hydrothermal Vent Fields on Alarcón Rise and in Southern Pescadero Basin, Gulf of California. *Geochem. Geophys. Geosyst.* **19**, 4788–4819 (2018).

132. Kawka, O. E. & Simoneit, B. R. T. Hydrothermal pyrolysis of organic matter in Guaymas Basin: I. Comparison of hydrocarbon distributions in subsurface sediments and seabed petroleums. *Organic Geochemistry* **22**, 947–978 (1994).

133. Lilley, M. D. *et al.* Anomalous CH4 and NH4+ concentrations at an unsedimented mid-ocean-ridge hydrothermal system. *Nature* **364**, 45–47 (1993).

134. You, C.-F. *et al.* Boron and halide systematics in submarine hydrothermal systems: Effects of phase separation and sedimentary contributions. *Earth and Planetary Science Letters* **123**, 227–238 (1994).

135. Proskurowski, G., Lilley, M. D. & Brown, T. A. Isotopic evidence of magmatism and seawater bicarbonate removal at the endeavour hydrothermal system. *Earth and Planetary Science Letters* **225**, 53–61 (2004).

136. Pedersen, R. B. *et al.* Discovery of a black smoker vent field and vent fauna at the Arctic Mid-Ocean Ridge. *Nat Commun* **1**, 126 (2010).

137. Baumberger, T. *et al.* Fluid composition of the sediment-influenced Loki's Castle vent field at the ultra-slow spreading Arctic Mid-Ocean Ridge. *Geochimica et Cosmochimica Acta* **187**, 156–178 (2016).

138. Charlou, J. L. *et al.* High production and fluxes of H2 and CH4 and evidence of abiotic hydrocarbon synthesis by serpentinization in ultramafic-hosted hydrothermal systems on the Mid-Atlantic Ridge. in *Geophysical Monograph Series 188* (eds. Rona, P. A., Devey, C. W., Dyment, J. & Murton, B. J.) vol. 188 265–296 (American Geophysical Union, 2010).

139. Andreani, M. *et al.* Tectonic structure, lithology, and hydrothermal signature of the Rainbow massif (Mid-Atlantic Ridge 36°14′N). *Geochem. Geophys. Geosyst.* **15**, 3543–3571 (2014).

140. Charlou, J. L., Donval, J. P., Fouquet, Y., Jean-Baptiste, P. & Holm, N. Geochemistry of high H2 and CH4 vent fluids issuing from ultramafic rocks at the Rainbow hydrothermal field (36°14′N, MAR). *Chemical Geology* **191**, 345–359 (2002).
141. Frost, B. R. On the Stability of Sulfides, Oxides, and Native Metals in Serpentinite. *Journal of Petrology* **26**, 31–63 (1985).
142. Abrajano, T. A. *et al.* Methane-hydrogen gas seeps, Zambales Ophiolite, Philippines: Deep or shallow origin? *Chemical Geology* **71**, 211–222 (1988).
143. McCollom, T. M., Klein, F., Solheid, P. & Moskowitz, B. The effect of pH on rates of reaction and hydrogen generation during serpentinization. *Phil. Trans. R. Soc. A.* **378**, 20180428 (2020).
144. McCollom, T. M. & Bach, W. Thermodynamic constraints on hydrogen generation during serpentinization of ultramafic rocks. *Geochimica et Cosmochimica Acta* **73**, 856–875 (2009).
145. Martin, W. & Russell, M. J. On the origin of biochemistry at an alkaline hydrothermal vent. *Phil. Trans. R. Soc. B* **362**, 1887–1926 (2007).
146. Martin, W., Baross, J., Kelley, D. & Russell, M. J. Hydrothermal vents and the origin of life. *Nat Rev Microbiol* **6**, 805–814 (2008).
147. Russell, M. J., Hall, A. J. & Martin, W. Serpentinization as a source of energy at the origin of life. *Geobiology* **8**, 355–371 (2010).
148. Hannington, M. D., De Ronde, C. E. J. & Petersen, S. Sea-Floor Tectonics and Submarine Hydrothermal Systems. in *One Hundredth Anniversary Volume* (Society of Economic Geologists, 2005). doi:10.5382/AV100.06.
149. Schmidt, K., Koschinsky, A., Garbe-Schönberg, D., de Carvalho, L. M. & Seifert, R. Geochemistry of hydrothermal fluids from the ultramafic-hosted Logatchev

hydrothermal field, 15°N on the Mid-Atlantic Ridge: Temporal and spatial investigation. *Chemical Geology* **242**, 1–21 (2007).

150. German, C. R. & Seyfried, W. E. Hydrothermal Processes. in *Treatise on Geochemistry* 191–233 (Elsevier, 2014). doi:10.1016/B978-0-08-095975-7.00607-0.

151. Seyfried, W. E., Pester, N. J., Ding, K. & Rough, M. Vent fluid chemistry of the Rainbow hydrothermal system (36°N, MAR): Phase equilibria and in situ pH controls on subseafloor alteration processes. *Geochimica et Cosmochimica Acta* **75**, 1574–1593 (2011).

152. Konn, C. *et al.* Extending the dataset of fluid geochemistry of the Menez Gwen, Lucky Strike, Rainbow, TAG and Snake Pit hydrothermal vent fields: Investigation of temporal stability and organic contribution. *Deep Sea Research Part I: Oceanographic Research Papers* **179**, 103630 (2022).

153. Thurnherr, A. M. & Richards, K. J. Hydrography and high-temperature heat flux of the Rainbow hydrothermal site (36°14′N, Mid-Atlantic Ridge). *J. Geophys. Res.* **106**, 9411–9426 (2001).

154. Canales, J. P., Dunn, R. A., Arai, R. & Sohn, R. A. Seismic imaging of magma sills beneath an ultramafic-hosted hydrothermal system. *Geology* **45**, 451–454 (2017).

155. Früh-Green, G. L. *et al.* Magmatism, serpentinization and life: Insights through drilling the Atlantis Massif (IODP Expedition 357). *Lithos* **323**, 137–155 (2018).

156. Proskurowski, G. *et al.* Abiogenic Hydrocarbon Production at Lost City Hydrothermal Field. *Science* **319**, 604–607 (2008).

157. Lang, S. Q., Butterfield, D. A., Schulte, M., Kelley, D. S. & Lilley, M. D. Elevated concentrations of formate, acetate and dissolved organic carbon found at the Lost City hydrothermal field. *Geochimica et Cosmochimica Acta* **74**, 941–952 (2010).

158. Proskurowski, G., Lilley, M. D., Kelley, D. S. & Olson, E. J. Low temperature volatile production at the Lost City Hydrothermal Field, evidence from a hydrogen stable isotope geothermometer. *Chemical Geology* **229**, 331–343 (2006).

159. Früh-Green, G. L. *et al.* 30,000 Years of Hydrothermal Activity at the Lost City Vent Field. *Science* **301**, 495–498 (2003).

160. Lang, S. Q. *et al.* Extensive decentralized hydrogen export from the Atlantis Massif. *Geology* **49**, 851–856 (2021).

161. Larson, B. I. *et al.* Stealth export of hydrogen and methane from a low temperature serpentinization system. *Deep Sea Research Part II: Topical Studies in Oceanography* **121**, 233–245 (2015).

162. Ternieten, L., Früh-Green, G. L. & Bernasconi, S. M. Carbonate Mineralogy in Mantle Peridotites of the Atlantis Massif (IODP Expedition 357). *Journal of Geophysical Research: Solid Earth* **126**, e2021JB021885 (2021).

163. Ternieten, L., Früh- Green, G. L. & Bernasconi, S. M. Distribution and Sources of Carbon in Serpentinized Mantle Peridotites at the Atlantis Massif (IODP Expedition 357). *JGR Solid Earth* **126**, e2021JB021973 (2021).

164. Kelemen, P. B. & Matter, J. In situ carbonation of peridotite for CO2 storage. *Proc. Natl. Acad. Sci. USA* **105**, 17295–17300 (2008).

165. Moore, W. S., Frankle, J. D., Benitez- Nelson, C. R., Früh- Green, G. L. & Lang, S. Q. Activities of ^{223}Ra and ^{226}Ra in Fluids From the Lost City Hydrothermal Field Require Short Fluid Residence Times. *JGR Oceans* **126**, (2021).

166. Kadko, D., Gronvold, K. & Butterfield, D. Application of radium isotopes to determine crustal residence times of hydrothermal fluids from two sites on the

Reykjanes Peninsula, Iceland. *Geochimica et Cosmochimica Acta* **71**, 6019–6029 (2007).

167. Kadko, D. & Butterfield, D. A. The relationship of hydrothermal fluid composition and crustal residence time to maturity of vent fields on the Juan de Fuca Ridge. *Geochimica et Cosmochimica Acta* **62**, 1521–1533 (1998).

168. Reeves, E. P. Timing Earth's Abiotic Kitchen: Short Hydrothermal Fluid Residence Times in Serpentinizing Oceanic Crust. *JGR Oceans* **127**, (2022).

169. Klein, F., Grozeva, N. G. & Seewald, J. S. Abiotic methane synthesis and serpentinization in olivine-hosted fluid inclusions. *Proc. Natl. Acad. Sci. U.S.A.* **116**, 17666–17672 (2019).

170. Etiope, G. & Whiticar, M. J. Abiotic methane in continental ultramafic rock systems: Towards a genetic model. *Applied Geochemistry* **102**, 139–152 (2019).

171. McCollom, T. M. & Seewald, J. S. Abiotic Synthesis of Organic Compounds in Deep-Sea Hydrothermal Environments. *Chem. Rev.* **107**, 382–401 (2007).

172. Kelley, D. S. & Früh-Green, G. L. Abiogenic methane in deep-seated mid-ocean ridge environments: Insights from stable isotope analyses. *J. Geophys. Res.* **104**, 10439–10460 (1999).

173. Kelley, D. S. & Früh-Green, G. L. Volatile lines of descent in submarine plutonic environments: insights from stable isotope and fluid inclusion analyses. *Geochimica et Cosmochimica Acta* **65**, 3325–3346 (2001).

174. Labidi, J. *et al.* Methane thermometry in deep-sea hydrothermal systems: Evidence for re-ordering of doubly-substituted isotopologues during fluid cooling. *Geochimica et Cosmochimica Acta* **288**, 248–261 (2020).

175. Wang, D. T., Reeves, E. P., McDermott, J. M., Seewald, J. S. & Ono, S. Clumped isotopologue constraints on the origin of methane at seafloor hot springs. *Geochimica et Cosmochimica Acta* **223**, 141–158 (2018).

176. Amend, J. P., McCollom, T. M., Hentscher, M. & Bach, W. Catabolic and anabolic energy for chemolithoautotrophs in deep-sea hydrothermal systems hosted in different rock types. *Geochimica et Cosmochimica Acta* **75**, 5736–5748 (2011).

177. Lang, S. Q. *et al.* Deeply-sourced formate fuels sulfate reducers but not methanogens at Lost City hydrothermal field. *Sci Rep* **8**, 755 (2018).

178. Lang, S. Q. & Brazelton, W. J. Habitability of the marine serpentinite subsurface: a case study of the Lost City hydrothermal field. *Phil. Trans. R. Soc. A.* **378**, 20180429 (2020).

179. Schrenk, M. O., Kelley, D. S., Bolton, S. A. & Baross, J. A. Low archaeal diversity linked to subseafloor geochemical processes at the Lost City Hydrothermal Field, Mid-Atlantic Ridge. *Environmental Microbiology* **6**, 1086–1095 (2004).

180. Adam, N. & Perner, M. Microbially mediated hydrogen cycling in deep-sea hydrothermal vents. *Frontiers in Microbiology* **9**, 1–17 (2018).

181. Mehta, M. P. & Baross, J. A. Nitrogen fixation at 92°C by a hydrothermal vent Archaeon. *Science* **314**, 1783–1786 (2006).

182. Brandes, J. A. *et al.* Abiotic nitrogen reduction on the early Earth. *Nature* **395**, 365–367 (1998).

183. Ménez, B. *et al.* Abiotic synthesis of amino acids in the recesses of the oceanic lithosphere. *Nature* **564**, 59–63 (2018).

184. Dasgupta, P. *The economics of biodiversity: the Dasgupta review: full report*. (HM Treasury, 2021).

185. Anderson, R. E. *et al.* Genomic variation in microbial populations inhabiting the marine subseafloor at deep-sea hydrothermal vents. *Nat Commun* **8**, 1114 (2017).

186. Poli, A. *et al.* Microbial diversity in extreme marine habitats and their biomolecules. *Microorganisms* **5**, 25 (2017).

187. Zeng, X., Alain, K. & Shao, Z. Microorganisms from deep-sea hydrothermal vents. *Mar Life Sci Technol* **3**, 204–230 (2021).

188. Cathalot, C. *et al.* Hydrothermal plumes as hotspots for deep-ocean heterotrophic microbial biomass production. *Nat Commun* **12**, 6861 (2021).

189. Anderson, R. E. Tracking Microbial Evolution in the Subseafloor Biosphere. *mSystems* (2021) doi:10.1128/mSystems.00731-21.

190. Spang, A. *et al.* Complex archaea that bridge the gap between prokaryotes and eukaryotes. *Nature* **521**, 173–179 (2015).

191. Eme, L., Spang, A., Lombard, J., Stairs, C. W. & Ettema, T. J. G. Archaea and the origin of eukaryotes. *Nat Rev Microbiol* **15**, 711–723 (2017).

192. Schleper, C. & Sousa, F. L. Meet the relatives of our cellular ancestor. *Nature* **577**, 478–479 (2020).

193. Williams, T. A., Cox, C. J., Foster, P. G., Szöllősi, G. J. & Embley, T. M. Phylogenomics provides robust support for a two-domains tree of life. *Nat Ecol Evol* **4**, 138–147 (2020).

194. McNichol, J. *et al.* Primary productivity below the seafloor at deep-sea hot springs. *Proc. Natl. Acad. Sci. U.S.A.* **115**, 6756–6761 (2018).

195. Thomas, E., Anderson, R. E., Li, V., Rogan, L. J. & Huber, J. A. Diverse Viruses in Deep-Sea Hydrothermal Vent Fluids Have Restricted Dispersal across Ocean Basins. *mSystems* **6**, 10.1128/mSystems.00068-21 (2021).

196. Hu, S. K. *et al.* Protistan grazing impacts microbial communities and carbon cycling at deep-sea hydrothermal vents. *Proc. Natl. Acad. Sci. U.S.A.* **118**, e2102674118 (2021).

197. Brazelton, W. J., Schrenk, M. O., Kelley, D. S. & Baross, J. A. Methane- and sulfur-metabolizing microbial communities dominate the Lost City Hydrothermal Feld ecosystem. *Appl Environ Microbiol* **72**, 6257–6270 (2006).

198. Brazelton, W. J. *et al.* Archaea and bacteria with surprising microdiversity show shifts in dominance over 1,000-year time scales in hydrothermal chimneys. *Proc. Natl. Acad. Sci. USA* **107**, 1612–1617 (2010).

199. Baross, J. A. & Members of the Ocean Memory Project. The Ocean Carries 'Memories' of SARS-CoV-2: We've been looking in the wrong place for a deeper understanding of the virus. *Scientific American* (2020).

200. Brazelton, W. J. & Baross, J. A. Abundant transposases encoded by the metagenome of a hydrothermal chimney biofilm. *ISME J* **3**, 1420–1424 (2009).

201. Brazelton, W. J., Mehta, M. P., Kelley, D. S. & Baross, J. A. Physiological differentiation within a single-species biofilm fueled by serpentinization. *mBio* **2**, 10.1128/mBio.00127-11 (2011).

202. Kodolányi, J., Pettke, T., Spandler, C., Kamber, B. S. & Gméling, K. Geochemistry of ocean floor and fore-arc serpentinites: Constraints on the ultramafic input to subduction zones. *Journal of Petrology* **53**, 235–270 (2012).

203. Elderfield, H. & Schultz, A. Mid-Ocean Ridge Hydrothermal Fluxes and the Chemical Composition of the Ocean. *Annu. Rev. Earth Planet. Sci.* **24**, 191–224 (1996).

204. Cannat, M., Cann, J. & Maclennan, J. Some Hard Rock Constraints on the Supply of Heat to Mid-Ocean Ridges. in *Geophysical Monograph Series* (eds. German, C. R., Lin, J. & Parson, L. M.) vol. 148 111–149 (American Geophysical Union, 2004).

205. Coogan, L. A. & Dosso, S. An internally consistent, probabilistic, determination of ridge-axis hydrothermal fluxes from basalt-hosted systems. *Earth and Planetary Science Letters* **323–324**, 92–101 (2012).

206. Drever JI. The Magnesium Problem. *Marine Chemistry* **5**, 337 (1974).

207. Edmond, J. M. *et al.* Ridge crest hydrothermal activity and the balances of the major and minor elements in the ocean: The Galapagos data. *Earth and Planetary Science Letters* **46**, 1–18 (1979).

208. Shalev, N., Bontognali, T. R. R., Wheat, C. G. & Vance, D. New isotope constraints on the Mg oceanic budget point to cryptic modern dolomite formation. *Nat Commun* **10**, 5646 (2019).

209. Luther, G. W. Hydrothermal Vents Are a Source of Old Refractory Organic Carbon to the Deep Ocean. *Geophys Res Lett* **48**, (2021).

210. Hansell, D. A. Recalcitrant Dissolved Organic Carbon Fractions. *Annu. Rev. Mar. Sci.* **5**, 421–445 (2013).

211. Druffel, E. R. M., Williams, P. M., Bauer, J. E. & Ertel, J. R. Cycling of dissolved and particulate organic matter in the open ocean. *J. Geophys. Res.* **97**, 15639 (1992).

212. Lang, S. Q., Butterfield, D. A., Lilley, M. D., Paul Johnson, H. & Hedges, J. I. Dissolved organic carbon in ridge-axis and ridge-flank hydrothermal systems. *Geochimica et Cosmochimica Acta* **70**, 3830–3842 (2006).

213. Hawkes, J. A. *et al.* Efficient removal of recalcitrant deep-ocean dissolved organic matter during hydrothermal circulation. *Nature Geosci* **8**, 856–860 (2015).

214. McCarthy, M. D. *et al.* Chemosynthetic origin of 14C-depleted dissolved organic matter in a ridge-flank hydrothermal system. *Nature Geosci* **4**, 32–36 (2011).

215. Lin, H.-T., Repeta, D. J., Xu, L. & Rappé, M. S. Dissolved organic carbon in basalt-hosted deep subseafloor fluids of the Juan de Fuca Ridge flank. *Earth and Planetary Science Letters* **513**, 156–165 (2019).

216. Shah Walter, S. R. *et al.* Microbial decomposition of marine dissolved organic matter in cool oceanic crust. *Nature Geosci* **11**, 334–339 (2018).

217. Druffel, E. R. M. *et al.* Dissolved Organic Radiocarbon in the Eastern Pacific and Southern Oceans. *Geophys Res Lett* **48**, (2021).

218. Früh-Green, G. L., Connolly, J. A. D., Plas, A., Kelley, D. S. & Grobéty, B. Serpentinization of oceanic peridotites: Implications for geochemical cycles and biological activity. in *Geophysical Monograph Series* (eds. Wilcock, W. S. D., DeLong, E. F., Kelley, D. S., Baross, J. A. & Craig Cary, S.) vol. 144 119–136 (American Geophysical Union, 2004).

219. Delacour, A., Früh-Green, G. L., Bernasconi, S. M., Schaeffer, P. & Kelley, D. S. Carbon geochemistry of serpentinites in the Lost City Hydrothermal System (30°N, MAR). *Geochimica et Cosmochimica Acta* **72**, 3681–3702 (2008).

220. Resing, J. A. *et al.* Basin-scale transport of hydrothermal dissolved metals across the South Pacific Ocean. *Nature* **523**, 200–203 (2015).

221. Lough, A. J. M. *et al.* Diffuse Hydrothermal Venting: A Hidden Source of Iron to the Oceans. *Frontiers in Marine Science* **6**, (2019).

222. Ardyna, M. *et al.* Hydrothermal vents trigger massive phytoplankton blooms in the Southern Ocean. *Nat Commun* **10**, 2451 (2019).

223. Schine, C. M. S. *et al.* Massive Southern Ocean phytoplankton bloom fed by iron of possible hydrothermal origin. *Nat Commun* **12**, 1211 (2021).

224. Kleint, C. *et al.* Trace Metal Dynamics in Shallow Hydrothermal Plumes at the Kermadec Arc. *Front. Mar. Sci.* **8**, 782734 (2022).

225. Guieu, C. *et al.* Iron from a submarine source impacts the productive layer of the Western Tropical South Pacific (WTSP). *Sci Rep* **8**, 9075 (2018).

226. Reese, B. K., Sobol, M. S., Bowles, M. W. & Hinrichs, K.-U. Redefining the subsurface biosphere: characterization of fungi isolated from energy-limited marine deep subsurface sediment. *Frontiers in Fungal Biology* **2**, 10.3389/ffunb.2021.727543 (2021).

227. Longnecker, K., Sievert, S. M., Sylva, S. P., Seewald, J. S. & Kujawinski, E. B. Dissolved organic carbon compounds in deep-sea hydrothermal vent fluids from the East Pacific Rise at 9°50′N. *Organic Geochemistry* **125**, 41–49 (2018).

228. Grandy, J. J., Onat, B., Tunnicliffe, V., Butterfield, D. A. & Pawliszyn, J. Unique Solid Phase Microextraction Sampler Reveals Distinctive Biogeochemical Profiles among Various Deep-Sea Hydrothermal Vents. *Sci Rep* **10**, 1360 (2020).

229. Noowong, A. *et al.* Imprint of Kairei and Pelagia deep-sea hydrothermal systems (Indian Ocean) on marine dissolved organic matter. *Organic Geochemistry* **152**, 104141 (2021).

230. Sert, M. F. *et al.* Compositions of dissolved organic matter in the ice-covered waters above the Aurora hydrothermal vent system, Gakkel Ridge, Arctic Ocean. *Biogeosciences* **19**, 2101–2120 (2022).

231. Kelley, D. S., Delaney, J. R. & Juniper, S. K. Establishing a new era of submarine volcanic observatories: Cabling Axial Seamount and the Endeavour Segment of the Juan de Fuca Ridge. *Marine Geology* **352**, 426–450 (2014).

232. Delaney, J. *et al.* Project NEPTUNE: An interactive, regional cabled ocean observatory in the northeast Pacific. *Proc. IEEE Oceans 2003, San Diego, CA* (2003).

233. Delaney, J. R. & Barga, R. S. *Observing the Oceans – A 2020 Vision for Ocean Science*. (Microsoft Research, 2009).

234. Petersen, S. *et al.* The geological setting of the ultramafic-hosted Logatchev hydrothermal field (14°45′N, Mid-Atlantic Ridge) and its influence on massive sulfide formation. *Lithos* **112**, 40–56 (2009).

235. Bach, W. & Früh-Green, G. L. Alteration of the Oceanic Lithosphere and Implications for Seafloor Processes. *Elements* **6**, 173–178 (2010).

236. Rouméjon, S., Cannat, M., Agrinier, P., Godard, M. & Andreani, M. Serpentinization and Fluid Pathways in Tectonically Exhumed Peridotites from the Southwest Indian Ridge (62-65°E). *Journal of Petrology* **56**, 703–734 (2015).

237. Rouméjon, S., Früh-Green, G. L., Orcutt, B. N., & the IODP Expedition 357 Science Party. Alteration heterogeneities in peridotites exhumed on the southern wall of the Atlantis Massif (IODP Expedition 357). *Journal of Petrology* **59**, 1329–1358 (2018).

238. Hentscher, M. & Bach, W. Geochemically induced shifts in catabolic energy yields explain past ecological changes of diffuse vents in the East Pacific Rise 9°50'N area. *Geochemical Transactions* **13**, 2 (2012).

239. Boetius, A. Lost City Life. *Science* **307**, 1420–1422 (2005).

240. Kelley, D. S., Delaney, J. R. & Team, C. A. NSF's Cabled Array: A wired tectonic plate and overlying ocean. in *OCEANS 2016 MTS/IEEE Monterey* 1–10 (IEEE, 2016). doi:10.1109/OCEANS.2016.7761398.

241. Nooner, S. L. & Chadwick, W. W. Inflation-predictable behavior and co-eruption deformation at Axial Seamount. *Science* **354**, 1399–1403 (2016).

242. Wilcock, W. S. D. *et al.* Seismic constraints on caldera dynamics from the 2015 Axial Seamount eruption. *Science* **354**, 1395–1399 (2016).

243. Barreyre, T. *et al.* Temporal variability and tidal modulation of hydrothermal exit- fluid temperatures at the Lucky Strike deep- sea vent field, Mid- Atlantic Ridge. *J. Geophys. Res. Solid Earth* **119**, 2543–2566 (2014).

244. Barreyre, T. & Sohn, R. A. Poroelastic response of mid- ocean ridge hydrothermal systems to ocean tidal loading: Implications for shallow permeability structure. *Geophys. Res. Lett.* **43**, 1660–1668 (2016).

245. Bohidar, S., Crawford, W. C. & Cannat, M. AGU Abstract V35A-0122 - Temporal and spatial evolution of seismicity at Lucky Strike volcano, Mid-Atlantic Ridge. (2021).

246. Miller, D. J., Iturrino, G. J. & Christensen. Geochemical and petrological constraints on velocity behavior of lower crustal and upper mantle rocks from the fast-spreading ridge at Hess Deep. *Proc. Ocean Drill. Program Sci. Results* **147**, 477–490 (1996).

247. Hirth, G., EscartíN, J. & Lin, J. The Rheology of the Lower Oceanic Crust: Implications for Lithospheric Deformation at Mid-Ocean Ridges. in *Geophysical Monograph Series* (eds. Roger Buck, W., Delaney, P. T., Karson, J. A. & Lagabrielle, Y.) vol. 106 291–303 (American Geophysical Union, 1998).

248. Boschi, C., Dini, A., Früh-Green, G. L. & Kelley, D. S. Isotopic and element exchange during serpentinization and metasomatism at the Atlantis Massif (MAR 30°N): Insights from B and Sr isotope data. *Geochimica et Cosmochimica Acta* **72**, 1801–1823 (2008).

249. Alt, J. C. & Shanks, W. C. Serpentinization of abyssal peridotites from the MARK area, Mid-Atlantic Ridge: sulfur geochemistry and reaction modeling. *Geochimica et Cosmochimica Acta* **67**, 641–653 (2003).

250. Andreani, M., Muñoz, M., Marcaillou, C. & Delacour, A. μXANES study of iron redox state in serpentine during oceanic serpentinization. *Lithos* **178**, 70–83 (2013).

251. Mayhew, L. E. & Ellison, E. T. A synthesis and meta-analysis of the Fe chemistry of serpentinites and serpentine minerals. *Phil. Trans. R. Soc. A.* **378**, 20180420 (2020).

Acknowledgements

G.F-G acknowledges support from the Swiss National Science Foundation (grant no. 200021-163187). Support to D.S.K. was provided by the US National Science Foundation grant no. OCE-0137206, the Management and Operation of the Ocean Observatories Initiative grant 1743430 and the University of Washington. M.D.L. was supported by the US National Science Foundation (grants OCE-1037874 and 535962) and the W.M. Keck Foundation for Project NEPTUNE. The authors acknowledge the late Karen L. Von Damm, who pioneered and inspired decades of MOR hydrothermal vent research discussed in this article. We further acknowledge the enthusiastic and unwaning efforts of John R. Delaney, who was instrumental in driving the innovative ideas behind installing seafloor observatories at JdF.

Author contributions

G.F-G coordinated and led the writing of this article; M.D.L. contributed to all aspects of writing, compiled data and led discussions on hydrothermal vent discoveries, distributions, fluid chemistry, volatiles and fluxes; D.S.K. led discussions on Axial, Endeavour, Ocean Observatories, phase separation and water-rock-microbe interactions, and together with her CEV team provided many of the figures; M.C. and V.C. provided input on slow- and ultraslow-spreading ridges and the EMSO observatory; J.A.B. wrote all sections on life in hydrothermal environments. All authors participated in discussions and edited multiple versions of the manuscript.

Competing interests

The authors declare no competing interests.

Peer review information

Nature Reviews Earth & Environment thanks [Referee#1 name], [Referee#2 name] and the other, anonymous, reviewer(s) for their contribution to the peer review of this work.

Data availability statement

The compilation of vent distributions and fluid compositions are provided in the online Supplementary Data file.

Supplementary information

Supplementary information is available for this paper at https://doi.org/10.1038/s415XX-XXX-XXXX-X

Related Links

Interactive Oceans - https://interactiveoceans.washington.edu

Ocean Networks - https://www.oceannetworks.ca/observatories/

European Multidisciplinary Seafloor and water-column Observatory (EMSO) - https://www.emso-fr.org/EMSO-Azores

Glossary

Chemosynthesis – The synthesis of organic compounds by microorganisms using energy derived from inorganic chemical reactions.

Oceanic crust – The outermost layer of the lithosphere formed at mid-ocean ridge (MOR) spreading centres; it is 5-10 km thick, primarily composed of mafic lavas, dikes and gabbros.

Gabbro – Igneous rock (formed from crystallization of magma) consisting primarily of varying proportions of the minerals plagioclase and pyroxene.

Peridotite – The dominant rock type in the Earth's upper mantle consisting primarily of the Mg-rich minerals olivine and pyroxene.

Lithosphere – Outer solid layer of the Earth, consisting of the brittle crust and uppermost mantle.

Asthenosphere – The viscous, mechanically weak and ductile region of the upper mantle between approximately 80 and 200 km depth that is involved in plate tectonic dynamics.

Spreading Rate – The rate at which new oceanic lithosphere is created at mid-ocean ridge plate boundaries resulting in seafloor spreading.

Oceanic crustal architecture – Rock types (lithologies), their distribution and structure of the oceanic crust.

Moho – The Mohorovičić discontinuity, known as the seismic Moho, is a discrete change in seismic wave velocities used to define the boundary between the crust and the mantle.

Ophiolite – Segments of oceanic crust and upper mantle tectonically exposed on land, often preserving features observed in different tectonic settings on the seafloor.

Oceanic detachment fault – Extensional normal fault associated with asymmetric spreading that results in exposure of lower crustal and upper mantle rocks on the seafloor.

Serpentinization – Hydrothermal process that transforms anhydrous Fe-Mg silicates into hydrous minerals, such as serpentine and brucite, producing magnetite and hydrogen.

Magma lens – During periods of enhanced magma replenishment at MORs, magma accumulates in an axial melt lens overlying smaller stacked sills beneath sheeted dikes.

Volatiles – Dissolved gases in hydrothermal fluids or exsolved from melts.

Hydrothermal plumes – Upwelling and dispersal of buoyant hydrothermal fluids into the ocean at hydrothermal vents or after eruptions or diking events.

Microbial floc – Microbial aggregates that appear as cloudy suspensions of cells floating in seawater rather than attached to a surface like most biofilms.

Snowblowers – A distinct form of low-temperature hydrothermal venting with expulsion of copious amounts of white flocculent microbial material, reminiscent of snow.

Critical point of seawater – Pressure and temperature conditions at which solid, liquid and vapour phases of seawater coexist in thermodynamic equilibrium.

pH – A logarithmic scale from 0-14 to indicate the concentration of hydrogen ions in an aqueous solution and specifies the acidity (pH <7) or basicity (pH>7) of the solution.

Abiotic – Formed or characterised by the absence of life or living organisms.

Aerobic – Pertaining to or requiring the presence of free oxygen.

Anaerobic – Occurring, living or active in the absence of free oxygen.

Heterotrophs – Organisms incapable of making their own food from light or inorganic compounds but consume complex organic compounds or other organisms in a food chain.

Hyperthermophilic – Pertaining to microorganisms that thrive in extremely hot environments and optimally grow above 80°C.

Display items

Table 1. | Summary of end-member hydrothermal system characteristics

	Sulphide Systems		Sediment-hosted & Sediment-Influenced Systems	Carbonate Systems (Lost City Type)
Host rock	**Hosted in basalt or gabbro**	**Hosted in gabbro and/or serpentinized peridotite**	**Hosted in basalt, sediment cover, or influenced by sediments at depth**	**Hosted in serpentinite (± gabbro)**
Heat source	Driven by cooling of magma / volcanic crust or gabbroic bodies	Driven by cooling of magma or gabbroic bodies; influenced by serpentinization	Driven by cooling of magma / volcanic crust; interaction with sediments along flow path	Driven by lithospheric cooling &influenced by serpentinization processes
Fluid temperature	High T: up to 400° C	High T: 300 - 360°C	High T: 280°- 320°C	Low-moderate T <120°C
pH	Low pH: 2-5	Low pH: 3-4	Moderate pH: 5-6	High pH: 10-11
Element enrichments	Enriched in metals (Fe, Cu, Mn, Zn, Pb) & Si	Enriched in metals (Fe, Cu, Mn, Zn) & variable Si	Variably enriched in metals, enriched in organic C	Low metal concentrations
Volatiles	High CO_2; variable H_2S, CH_4, H_2	High CO_2, CH_4, H_2 & organic compounds; variable H_2S	High CH_4, NH_4^+; variable H_2S, CO_2, H_2	High H_2, CH_4, C2-C4's & organic acids; variable H_2S; negligible CO_2
Type of hydrothermal deposits	Metal-sulphide chimneys & stockworks in basement	Metal-sulphide chimneys & stockworks in basement	Metal-sulphide chimneys & stockworks in basement	Carbonate-brucite chimneys & carbonate in basement
Venting characteristics	-> Black & white smokers	-> Black (& white) smokers	-> Black & white smokers	*-> Not "white" smokers* Clear "non-smoking" fluids

Note: Compilation of vent distributions and fluid compositions in Supplementary Data.

Figures

Fig. 1 | **Global distribution of hydrothermal vents on the seafloor**. Map of the global ridge system with distribution of known sites of hydrothermal venting and sites inferred to be present from water column studies. Hydrothermal vents occur at MORs (red dots, 65% of known sites), back arc spreading centres (purple dots, 22%), and submarine arc volcanoes (yellow dots, 1%). Data from the InterRidge Vents Database. Map produced by the Center for Environmental Visualization, University of Washington (CEV, UW).

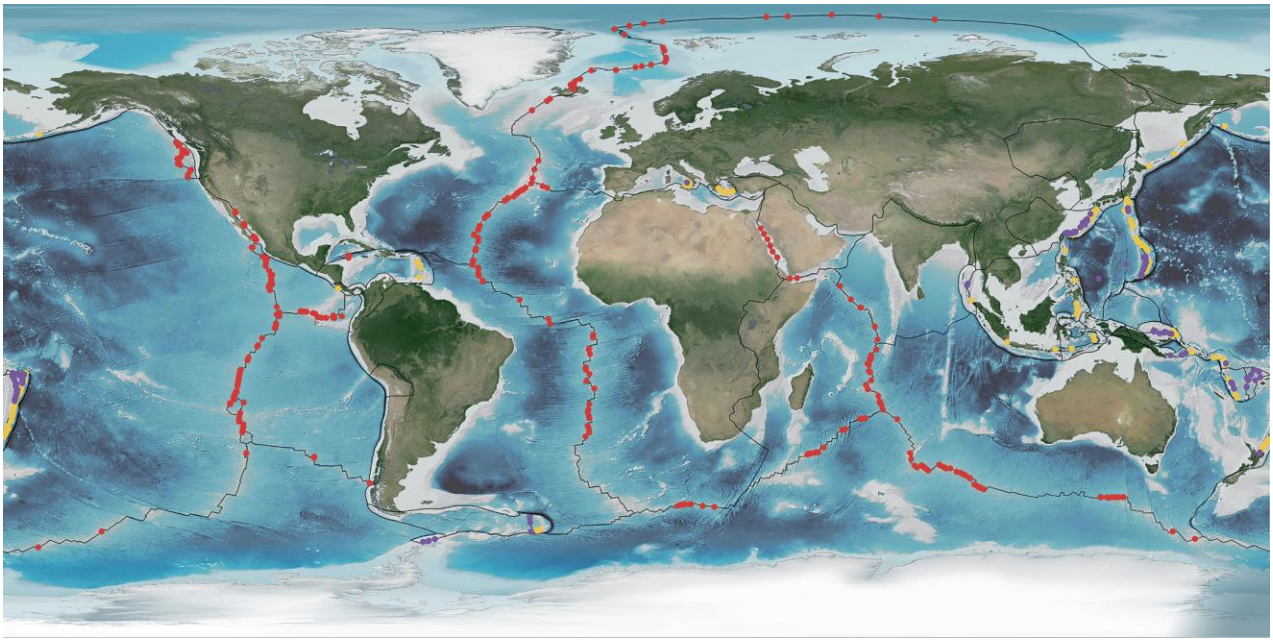

Fig. 2 | **Variations in magmatism, structure and hydrothermal systems with varying spreading rates.** Conceptual, across-axis comparison with variations in magmatism and spreading rate. **a**| Regions with phases of robust magmatism, characteristic of fast spreading MORs, produce a relatively homogeneous layered crust. Geophysical models predict that sub-Moho melts feed sills through small dikes and accumulate in a shallow axial melt lens (AML), producing stacked sills and a crystal mush zone (high melt %; stippled region) surrounded by hot gabbroic rock[23]. A conductive boundary layer (CBL) separates the AML from hydrothermal circulation where focused fluid flow produces high temperature Type-1 vent fields. Depth of profile ~6 km. **b** | Slow-spreading ridges are heterogenous and influenced by discontinuous magmatism leading to detachment faults, asymmetric ridge segments, and oceanic core complexes (OCC). Detachment faults can channel high-temperature Type 1 fluids (such as at TAG[63,76,148]) and drive flow in gabbro- and peridotite-influenced Type 2 hydrothermal systems (such as at Logatchev and Rainbow[139,140,234]). Late normal faults can focus low-temperature, alkaline fluids (Type 3 fluids, blue arrows) leading to large carbonate deposits, as at Lost City[65,80]. Depth of profile ~9 km. **c** | Types of hydrothermal vents types described in panels **a** and **b**. **d** | The structure named Sully on the Endeavour Segment, Juan de Fuca ridge, overgrown with *Ridgeia piscesae* tubeworms venting 380°C Type 1 black smoker fluids after a diking event in 1999-2000. **e** | The black smoker structure named Candelabra, venting Type 2 fluids at a water depth of 3,300 metres in the Logatchev Hydrothermal Field, MAR. **f** | Carbonate-brucite deposits at 845 m water depth at the Lost City hydrothermal field, MAR 30°N. Supplementary Videos. Panel a adapted with permission from REF.[23]. Panel b modified with permission from REFS[49,79,235]. Panel d credit: Delaney, J.R. and Kelley, D.S, University of Washington; Canadian Scientific Facility - ROV ROPOS, 2004; W.M. Keck Foundation. Panel e credit: MARUM – Center for Marine Environmental Sciences, University of

Bremen (CC-BY 4.0). Panel f credit: D.S. Kelley, UW, URI-ROV Hercules, IFE, URI-IAO, Lost City Science Party 2005, & NOAA Ocean Exploration.

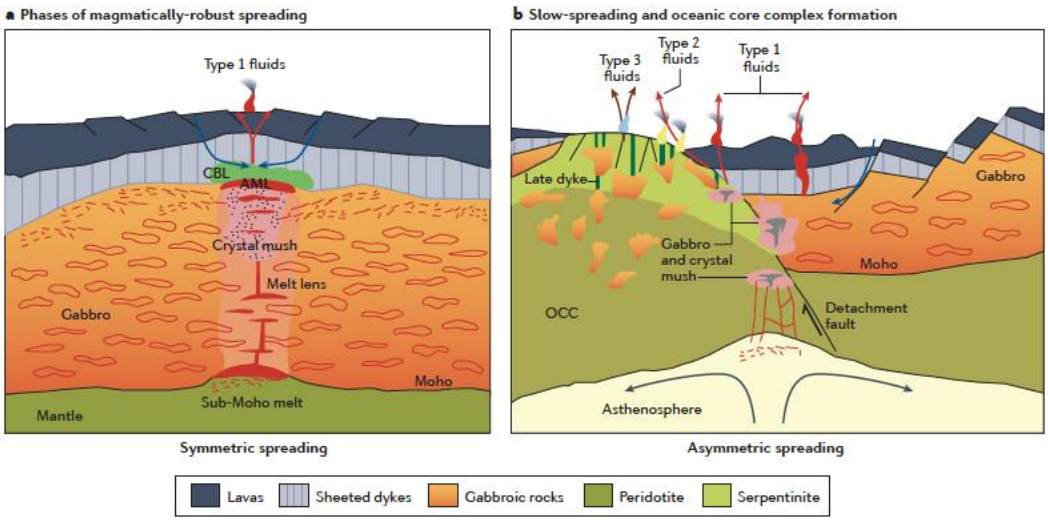

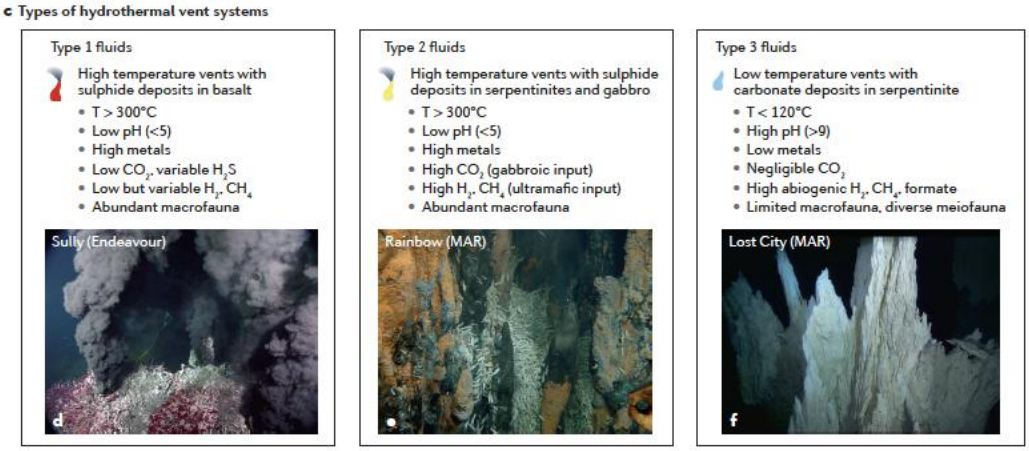

Fig. 3 | **Hydrothermal processes at mid-ocean ridges. a |** Summary of factors that influence hydrothermal activity and fluid chemistry at MORs. **b |** Conceptual sketch of water-rock reactions and flow paths in an idealised basalt-hosted seafloor hydrothermal system[31,87]. Hot fluids rise buoyantly to the seafloor, where metal-rich, superheated fluids are expelled into the ocean, precipitating metals and forming black and white smoker edifices. **c**| Plot of maximum measured temperatures and pressures of fluids issuing from hydrothermal vents (Supplementary Data). The two-phase boundary (black line) and critical point (large red dot at 407°C, 298 bar) of seawater[97] are shown with labels indicating the boiling and condensation fields. Inset diagrams show how volatiles partition preferentially into the less dense phase[31,97]. Inset image is of magmatic fluid inclusions (700°C) in gabbros from the MARK area[98]. Panel b credit: D.S. Kelley, J.R. Delaney, CEV, UW.

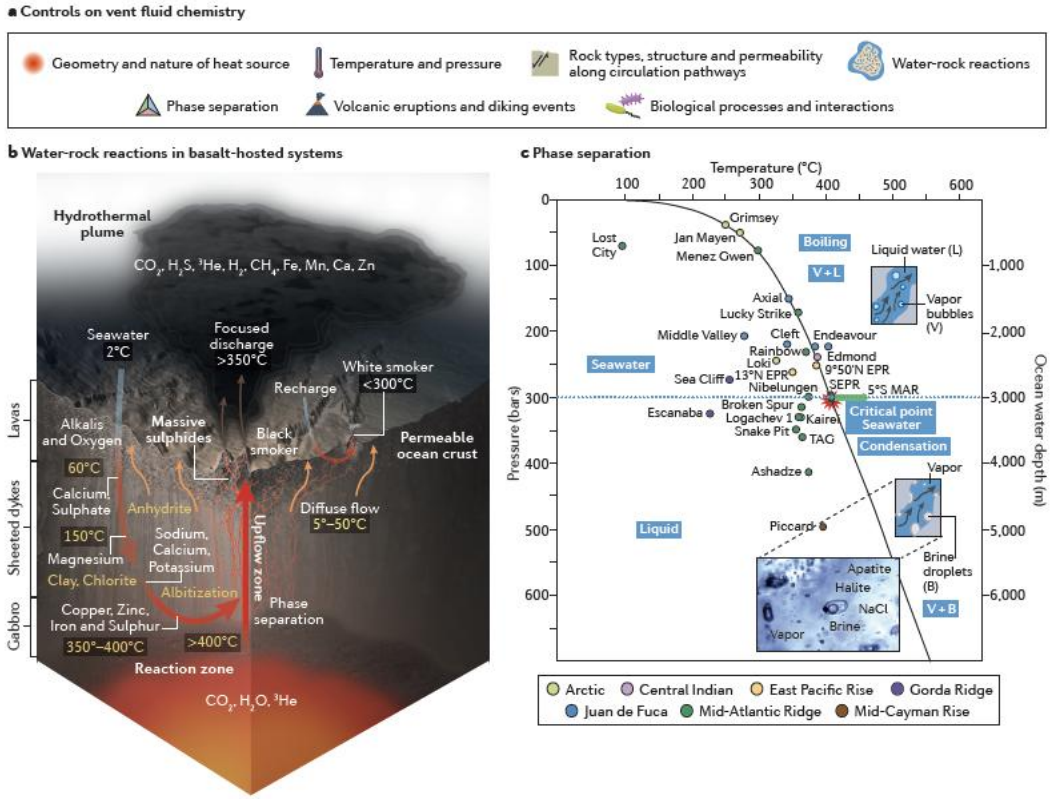

Fig. 4 | **Mid-ocean ridge hydrothermal fluxes and life**. **a** | Variations in availability of electron donors and electron acceptors under varying temperature and redox conditions and their potential metabolic energy sources. Examples of general inorganic redox reactions along thermochemical mixing gradients in vent environments that support diverse microbial communities, with potential locations along subsurface flow paths in basalt-hosted systems shown as circled numbers on panel **b**. **b** | Representation of fluid flow paths and fluid-rock interactions that govern chemical fluxes, redox reactions and microbial ecosystems at magmatically robust black smoker systems with circulation limited to the upper crust (<2-3 km) above axial magma lenses. Reactions 1–4 take place in the shallow subsurface and zones of mixing with seawater and are not restricted to any particular distance from the ridge axis. **c** | Same as **b**, but for a Lost City-type system controlled by faults and serpentinization processes (BOX 2). Light blue anastomosing network depicts early interconnected fluid pathways leading to the onset of serpentinization[162,236]. Reactions between gabbro lenses and peridotite cause localised silica metasomatism (lightest green patches in serpentinized domains)[155,237]. Panel b modified after REF [238]. Inset in 4b modified after REF[96] . Panel c modified after REFS[155,162,237]; inset modified after REF[239].

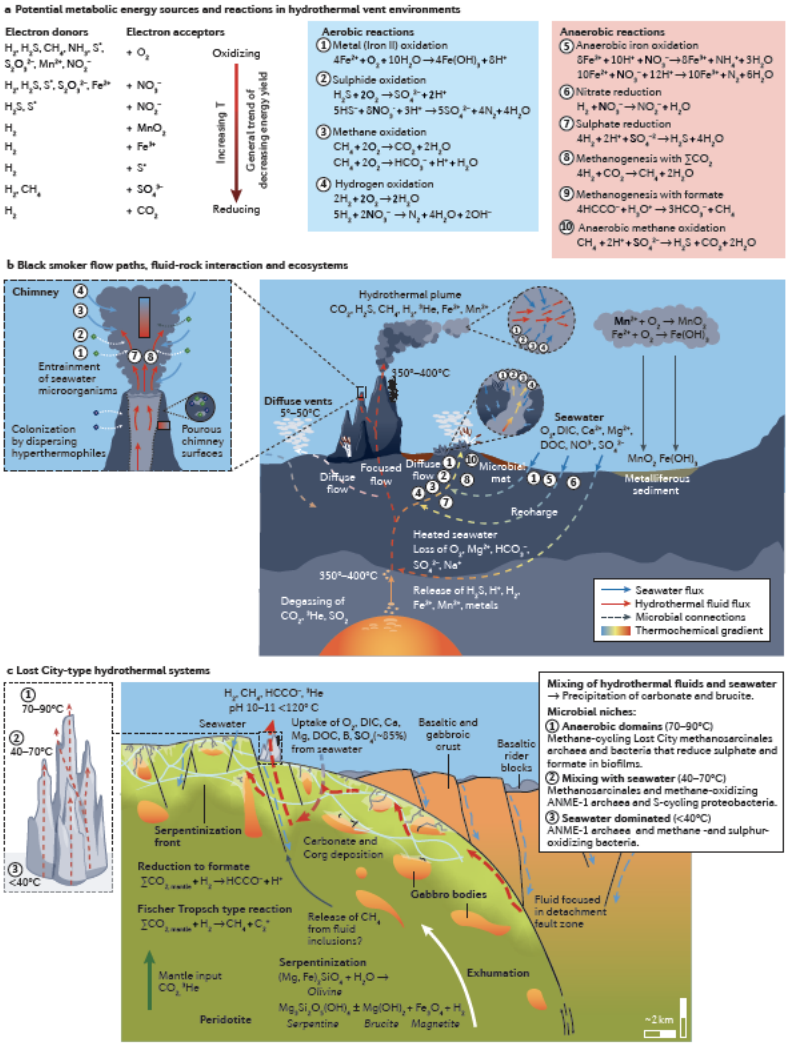
a Potential metabolic energy sources and reactions in hydrothermal vent environments
Electron donors
Electron acceptors
Oxidizing
Increasing T
General trend of decreasing energy yield
Reducing
Aerobic reactions
1 Metal (iron II) oxidation
2 Sulphide oxidation
3 Methane oxidation
4 Hydrogen oxidation
Anaerobic reactions
5 Anaerobic iron oxidation
6 Nitrate reduction
7 Sulphate reduction
8 Methanogenesis with ΣCO2
9 Methanogenesis with formate
10 Anaerobic methane oxidation
b Black smoker flow paths, fluid-rock interaction and ecosystems
Chimney
Entrainment of seawater microorganisms
Colonization by dispersing hyperthermophiles
Porous chimney surfaces
Hydrothermal plume
Diffuse vents
Seawater
Diffuse flow
Focused flow
Microbial mat
Metalliferous sediment
Recharge
Heated seawater
Degassing of
Seawater flux
Hydrothermal fluid flux
Microbial connections
Thermochemical gradient
c Lost City-type hydrothermal systems
70–90°C
40–70°C
<40°C
Seawater
Uptake of
Basaltic and gabbroic crust
Basaltic rider blocks
Serpentinization front
Carbonate and Corg deposition
Reduction to formate
Fischer Tropsch type reaction
Release of CH4 from fluid inclusions?
Gabbro bodies
Fluid focused in detachment fault zone
Exhumation
Mantle input
Serpentinization
Olivine
Peridotite
Serpentine
Brucite
Magnetite
~2 km
Mixing of hydrothermal fluids and seawater → Precipitation of carbonate and brucite.
Microbial niches:
1 Anaerobic domains (70–90°C)
Methane-cycling Lost City methanosarcinales archaea and bacteria that reduce sulphate and formate in biofilms.
2 Mixing with seawater (40–70°C)
Methanosarcinales and methane-oxidizing ANME-1 archaea and S-cycling proteobacteria.
3 Seawater dominated (<40°C)
ANME-1 archaea and methane -and sulphur-oxidizing bacteria.

Boxes

[B1] BOX 1 | Ocean observatories

Ocean floor observatories have advanced the ability to study interactions of seafloor deformation, volcanism, hydrothermal circulation and microbial activity during ocean crust evolution. Below we provide a brief overview of three ocean observatories currently installed to study MOR processes:

Regional Cabled Array (RCA) and Ocean Networks Canada (ONC) – combined***,*** these two instrumented networks on the Juan de Fuca Ridge form the first submarine cabled observatories to monitor an entire tectonic plate. The mid-ocean ridge components of the two observatories focus on both the magmatically robust Axial Seamount (RCA, operated by the U.S.), which erupted in 1998, 2011, and 2015, and the tectonically active Endeavour Segment (ONC, operated by Canada)[231,240] (see figure). These two networks are linked to the global internet and provide data and imagery in real- to near-real time. Continuous monitoring of the oceanic plate is made possible through ~1700 km of fibre optic cable and 14 subsea terminals that provide 8-10 kW power and 10 Gbs two-way communications to hundreds of instruments on the seafloor and in the water column. A highlight of the networked RCA was the live detection of the 2015 Axial Seamount eruption, marked by a seismic crisis of >8,000 earthquakes coincident with 2.4 m of seafloor subsidence over a 24 hour period[241]. Hydrophones detected acoustic activity delineating more than 30,000 volcanic explosions as lava spilled onto the seafloor[242], culminating in a 127 m-thick submarine lava flow. Three months later the summit of the flow was covered by kilometres of microbial mats fed by nutrient-rich, warm fluids circulating through the cooling lava[119].

European Multidisciplinary Seafloor and water-column Observatory (EMSO) – is located on the Mid-Atlantic Ridge south of the Azores. The principal target of the uncabled EMSO is to

understand shorter-term variations of the Lucky Strike hydrothermal system in a tectonically complex framework, and their impact on life at and beneath the seafloor, similar to the JdF sites. One observatory node of the EMSO infrastructure is dedicated to long-term (>20 years) monitoring of volcanic, tectonic, hydrothermal and biological activity at Lucky Strike[67]. The observatory includes arrays of autonomous instruments and two stations that communicate acoustically to a surface-relay buoy which transmits data to shore every 6 hours. Two stations monitor seismic activity, pressure at the seafloor, and key environmental parameters; one of these stations also connects to a camera that records daily videos of the hydrothermal fauna. Monitoring of variable responses to tidal forcing has revealed changes in the subseafloor permeability structure[243,244] and episodic increases in microseismic activity. Changes in earthquake locations through time indicate that the main heat extraction is to the north of the hydrothermal field and moved by about 800m to the east between late 2013 and late 2015[245].

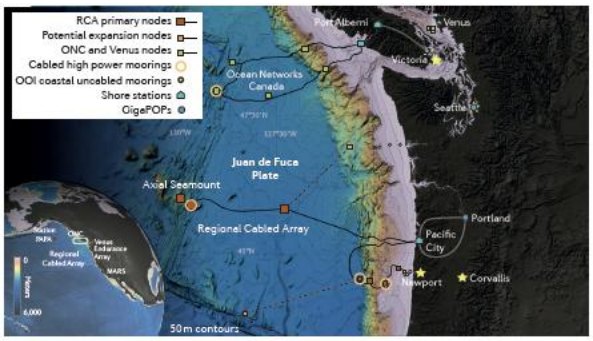

[B2] Box 2 | **Serpentinization and volatiles in the oceanic lithosphere**

The discovery of hydrothermal vents influenced by serpentinized ultramafic upper mantle rocks – and in particular, the discovery of the off-axis Lost City vent field – has had a key impact on the overall understanding of the role of slow-spreading ridges in global hydrothermal fluxes and the potential impacts of serpentinization[218] (FIG. 4c).

Serpentinization involves hydration of mantle olivine and pyroxene, which produces hydrogen and incorporates up to 14 wt. % H_2O. Serpentinization decreases bulk density (to 2.5-2.9 g cm^{-3}) and seismic velocities (Vp <6 km s^{-1}), and directly affects the strength and physical properties of the mantle, and the magnetic and gravity signatures of the oceanic lithosphere[246,247]. The depth to which serpentinization can occur is controlled by the depth to which seawater can penetrate into the oceanic lithosphere and is largely controlled by tectonic processes and fracture permeabilities. The depth and spatial extent of serpentinized oceanic peridotites has direct consequences for the interpretation of seismic velocity data and can influence where geophysicists estimate the location of the seismic Moho. In addition, the presence of gabbroic intrusions in mantle peridotites leads to Si mobility and talc formation during alteration, which can influence the strength of the lithosphere along detachment faults and aid in uplift and emplacement of mantle sequences at the seafloor.

Serpentinization reactions are associated with the uptake or release of many components, such as H_2O, Mg, Ca, Si, Cl, Li, B, C, and S[218,237,248,249], which can be recycled through subduction and affect subduction zone dynamics and the compositions of arc magmas[202]. In addition, serpentinization reactions lead to highly reduced fluids with high concentrations of H_2, which distinguishes peridotite-hosted systems from basalt-dominated or sediment-influenced systems (see figure and Supplementary Data). Hydrogen production is linked to oxidation of ferrous iron

in mantle minerals to produce magnetite during serpentinization, which is limited by brucite formation and incorporation of Fe in other alteration phases in oceanic serpentinites[218,250,251].

Fluids in serpentinizing environments characteristically have elevated concentrations of methane, formate, ethane, propane, and other straight chain hydrocarbons[152,156,177]. H_2 production and the formation of organic molecules and reduced C-species have been considered to form through abiotic reactions, catalysed by Fe-, Ni-, and Cr-bearing minerals, and have important consequences for global chemical cycles and biological activity on and within the seafloor[218]. The geochemical reactions that occur during serpentinization could have been key in early biochemical evolution, which potentially has major implications for the origin and evolution of life on Earth and other planets[145–147].